Mathematical and Computational Applications

MDPI

Article

Sliding Mode Fault-Tolerant Control for Nonlinear LPV Systems with Variable Time-Delay

Omayma Mansouri *, Ali Ben Brahim, Fayçal Ben Hmida and Anis Sellami

Engineering Laboratory of Industrial Systems and Renewable Energies (LISIER), National Higher Engineering School of Tunis (ENSIT), University of Tunis, 5 Avenue Taha Hussein, Tunis BP 56-1008, Tunisia; benibrahimmali@yahoo.fr (A.B.B.); faycal.benhmida@ensit.rnu.tn (F.B.H.); anis.sellami@ensit.rnu.tn (A.S.)

* Correspondence: mansouri1omayma@gmail.com

Abstract: This paper presents a robust sliding mode fault-tolerant control (FTC) strategy for a class of linear parameter variant (LPV) systems with variable time-delays and uncertainties. First fault estimation (FE) is conducted using a robust sliding mode observer, synthesized to simultaneously estimate the states and actuator faults of LPV polytopic delayed systems. Second, a sliding mode FTC is developed, ensuring all states of the closed-loop system converge to the origin. This paper presents an integrated sliding mode FTC strategy to achieve optimal robustness between the observer and controller models. The integrated design approach offers several advantages over traditional separated FTC methods. Our novel approach is based on incorporating adaptive law into the design of the Lyapunov–Krasovskii functional to improve both robustness and performance. This is achieved by combining the concept of sliding mode control (SMC) with the Lyapunov–Krasovskii function under the H_∞ criteria, which plays a key role in guaranteeing the stability of this class of system. The effectiveness of the proposed method is demonstrated through a diesel engine example, which highlights the validity and benefits of the integrated and separated FTC strategy for uncertain nonlinear systems with time delays and the sliding mode control.

Keywords: fault estimation (FE); LPV delayed systems; fault-tolerant control (FTC); Lyapunov–Krasovskii functional; multi-objective LMI

Citation: Mansouri, O.; Ben Brahim, A.; Ben Hmida, F.; Sellami, A. Sliding Mode Fault-Tolerant Control for Nonlinear LPV Systems with Variable Time-Delay. *Math. Comput. Appl.* **2024**, *29*, 96. https://doi.org/10.3390/mca29060096

Academic Editor: Guillermo Valencia-Palomo

Received: 22 September 2024
Revised: 18 October 2024
Accepted: 20 October 2024
Published: 26 October 2024

1. Introduction

LPV systems with time delays have received limited attention in the literature. However, only a few contributions have been reported, reflecting much more potential for future study and an interesting research area. From each system class, these systems come with many challenges and offer new problems. For instance, the implemented technique for both robust control and LPV could no longer be used in the context of LPV systems with delays. For this system class, especially for parameter-varying time delays, there are some problems, such as actuator degradation, sensor/actuator failures, and output measurement variations. These are the things that contribute to the disturbance in system operation, and from them, both poor controller performance and system deterioration follow. These issues disrupt system operation, leading to poor controller performance or system deterioration. This has led to the exploration of fault-tolerant control design [1], specifically tailored to LPV systems with time delays. Therefore, to prevent poor system performance and potential collapse or failure, FTC design has emerged. First, it ensures closed-loop stability in the presence of disturbances or uncertainties, particularly in passive FTC configurations, and second, it provides much more reliability and supervision when in active FTC setups.

The effectiveness of the FTC is highly dependent on the accuracy of the fault detection and isolation (FDI). If faults are detected quickly and accurately, the FTC can be applied more effectively to mitigate their impact. Ref. [2] presents a new two-stage framework for FDI in quadrotors, with a particular focus on actuator faults. This model-based method uses a parity space approach to generate residual signals for fault detection, taking advantage of measurement consistency through linear combinations of measurement outputs and control inputs. Faulty system states are filtered using an extended Kalman filter, improving the accuracy of state estimates and the overall performance of the fault detection algorithm.

In [3–6], the authors propose a robust active FTC for uncertain LPV systems with simultaneous actuator and sensor faults. The researchers in [7] presented a robust fault-tolerant control methodology tailored to discrete-time LPV systems. The methodology focuses on the synthesis of a reconfiguration block comprising virtual sensors and virtual actuators. The aim is to address the issue of fault-tolerant sensor control by proposing a model-free, adaptive constrained control strategy that utilizes virtual sensor technology [8,9]. To maintain system performance and stability, active FTC control can automatically integrate faulty components. Nevertheless, fault estimation presents design challenges, and the applicability of the suggested approaches is limited. One fault estimation technique that is widely employed, as in [10,11], involves estimation by sliding mode observers (SMOs).

However, their application is mainly limited to specific types of nonlinear systems, such as nonlinear LPV delayed systems. The fault estimation technique only identifies the fault size but does not provide a guide on how to compensate for its effects. Compared to FDI, fault estimation presents more design challenges [12]. Additionally, using the information obtained from the estimator, an additive controller can be designed to compensate for the effect of the fault. The design of fault estimation based on the sliding mode observer typically requires a strictly positive real state to be satisfied. Several studies have proposed fault estimation and FTC approaches based on sliding mode observers for various types of nonlinear systems [13–15]. However, the application of sliding mode FTC methods is essentially limited to certain specific types of nonlinear systems, such as nonlinear LPV systems with delays. The fault estimation provides the magnitude of the fault but does not indicate how to mitigate its effects, thus highlighting the need for the fault-tolerant control step. This step involves developing a control law that can maintain or ensure stability and acceptable performance, even when the LPV system is impacted by the fault. While there are many references in the literature dealing with the problem of active fault-tolerant control for LPV systems, most of them concern linear systems [16,17]. However, due to the nonlinear behavior of most real systems, the application of FTC must consider the nonlinear nature of these systems [4,8] and recently in [18,19]. On the other hand, variable delays and uncertainties are common in many practical applications, which can also contribute to the degradation of system performance. The presence of a delay with a fault can easily destabilize the system [20,21]. Therefore, the research on the fault-tolerant control problem for nonlinear LPV systems with time delay is of great interest, both from theoretical and practical perspectives.

The author in [22] focuses on the problem of in-memory state feedback control for Takagi-Sugeno type 2 fuzzy systems with time delay, particularly dealing with external disturbances and actuator faults. The use of Takagi-Sugeno type 2 fuzzy systems highlights the importance of managing uncertainties and the occurrence of faults in the system. This allows the system to use information from previous states, which can potentially improve control performance. Intensive research attention focuses on sliding mode controllers (SMCs). The researchers in [23] introduced a new adaptive fixed-time fractional integral control strategy that combines the advantages of fractional calculus with robust control techniques. Recently, Ref. [24] introduced advanced control strategies for nonlinear systems through a fixed-time adaptive control approach. This method combines rapid convergence, smooth control inputs, and robust performance in the presence of external disturbances. This method guarantees that stability is achieved within a predetermined time frame, regardless of the initial conditions.

Motivated by previous works, this study primarily aims to reconfigure a robust sliding mode controller to maintain closed-loop system stability with acceptable performance, despite the presence of actuator faults, variable time-delay, and uncertainties.

This paper proposes a fault estimation based on a sliding mode fault-tolerant control (FTC) scheme for a class of nonlinear LPV delayed systems subject to actuator faults and uncertainty. The LPV delayed system modeling with local nonlinear models, as Lipschitzian nonlinearities, is of great interest in this work. Compared to existing results, the main contributions of this paper are divided as follows:

- First, a sliding mode observer is designed for the uncertain polytopic system with local nonlinearities and variable time-delays, enabling the simultaneous reconstruction of system states and actuator faults. The sliding mode observer designed for this class of system offers significant advantages in terms of robustness, adaptability, and performance. It is capable of simultaneously estimating state and faults while effectively managing variable time-delays. By exploiting these strengths, this approach improves not only the reliability of systems but also opens up the prospect of progress in the field of FTC methodologies.
- Second, we propose an SMC method with an adaptive law that has many advantages over other approaches, including uncertain LPV systems with local non-linearities and variable time-delay. By incorporating an adaptive law, the control strategy can be regularly modified in response to the system's real-time returns. For systems with high levels of uncertainty or non-linearity, adaptability is necessary to maintain maximum performance. Indeed, the adaptive law may also help to address the conversational phenomenon generally associated with traditional sliding mode control strategies.
- Third, the combination of FE and FTC design within a unified framework is developed for the delayed polytopic system, aiming to achieve optimal robustness and performance. Compared to constant time delay systems, variable time-delay in FE and FTC models presents additional challenges in the polytopic system. This framework is specifically designed to deal with variable time-delays, which are common in practical applications. By accounting for these delays in FE and FTC processes, the system can maintain accurate state estimates and effective control actions, improving overall reliability. Moreover, the proposed method effectively addresses these challenges by taking into account the presence of local non-linearities and uncertainties. It ensures that the control strategy remains effective even when the system dynamics change. On the other hand, this methodology allows for the simultaneous estimation of actuator faults and the implementation of control laws. Therefore, when faults are detected, the FTC system can dynamically adjust control actions to minimize their impact on the system's performance.
- Finally, the integrated FE-FTC framework is formulated for the uncertain polytopic system with local nonlinear models, which combines the observer and controller synthesis into a single optimization problem. The integrated FE-FTC scheme is designed to maintain stability even in the presence of variable time-delays. By jointly optimizing the control and estimation strategies, the system can adapt to variations in delay. This approach offers greater robustness and better performance than traditional separated FE-FTC methods. The advantages of the proposed methods for this class of complex systems are demonstrated to prove the performance of integrated and separate FTC approaches through a case study involving an uncertain polytopic system with local nonlinear models and variable delays.

In [25,26], the researchers developed a sliding mode observer (SMO) with unknown inputs for descriptor systems (LPVs) with variable delays, which have several drawbacks compared to our approach, such as the sensitivity of the unknown inputs. This sensitivity can lead to performance degradation and instability, particularly in LPV-delayed systems. SMOs with unknown inputs cannot effectively compensate for these delays, leading to inaccurate state estimates and control actions that can destabilize the system. The authors have only used the state feedback to compute the control law. As a result, the efficiency of the SMO used may be limited by the complex local non-linearities present in polytopic delayed systems. The inability to manage these nonlinearities adaptively can lead to non-optimal performance. Compared to our study, the adaptive nature of the SMC designed in this paper is often more robust to input variations and nonlinearities, particularly local Lipchitz nonlinearity. This allows problems to be quickly identified and corrected as they arise. The ability to adjust parameters dynamically enables better fault detection and state estimation. Moreover, when designing control law with an emphasis on fault tolerance and estimation, it is essential to find a trade-off between robustness and computational efficiency. The adaptive aspect of our SMC provides a strong framework for ensuring system stability despite these changes. This is achieved by combining the concept of sliding mode control (SMC) with the Lyapunov–Krasovskii function under the H_∞ criteria, highlighting two approaches for fault-tolerant control (FTC) design: integrated FTC and separated FTC. These play a crucial role in ensuring the stability and robustness of this class system. Our integrated approach ensures this trade-off by performing fault estimation and fault-tolerant control in a single step, thereby reducing computational complexity.

The structure of the rest of this paper is as follows: Section 2 presents an overview of the non-linear delayed LPV system. More details of the LPV adaptive observer design are presented in Section 3. Section 4 then outlines the structure of the sliding mode controller. In Section 5, we introduce the separate and integrated sliding mode FTC schemes to stabilize the closed-loop system. Section 6 presents a simulation example based on non-linear simulations, demonstrating the effectiveness of the proposed schemes with comparative studies to highlight the advantages of our approach. Finally, Section 7 presents our concluding remarks.

2. Problem Formulation

Consider an uncertain nonlinear system governed by the following equations:

$$\begin{aligned}
\dot{x}(t) &= \varphi_{x1}(x(t)) + \varphi_{x2}(x(t))x(t-d(t)) + \varphi_{x3}(x(t))u(t) + \varphi_{x4}(x(t))\xi(x,t) \\
&+ \varphi_{x5}(x(t))\Gamma(x,t) + \varphi_{x6}(x(t))f(t) \\
y(t) &= \varphi_2(x(t)) \\
y_L(t) &= \varphi_{yl}(x(t))
\end{aligned} \tag{1}$$

System (1) is written with the following polytopic representation:

$$\begin{aligned}
\dot{x}(t) &= \sum_{i=1}^{g} \mu_i(\theta(t))A_i x(t) + A_{di}x(t-d(t)) + B_i u(t) &(2)\\
&+ D_i\xi(t,x) + \Gamma_i(x,u) + M_i f_a(t)\} \\
y(t) &= \sum_{i=1}^{g} \mu_i(\theta(t))\{C_i\, x(t)\} &(3)
\end{aligned}$$

where $x(t) \in \Re^n$ represents the state vector, $y(t) \in \Re^p$ represents the measurement, $u(t) \in \Re^m$ represents the input, $f_a(t) \in \Re^q$ represents the actuator fault, and $\xi(t) \in \Re^l$ encompasses the uncertainty. This uncertainty represents the unknown and bounded uncertainties that are part of $L_2 \in \begin{bmatrix} 0 & \infty \end{bmatrix}$. The functions $\varphi_{xi}(x(t))$, $\varphi_2(x(t))$, $\varphi_{yl}(x(t))$, and $\Gamma(x,t)$ are continuously nonlinear, with $i = 1,2,3,4,5$.

$A_i \in \Re^{n\times n}$, $A_{di} \in \Re^{n\times n}$, $B_i \in \Re^{n\times m}$, $M_i \in \Re^{n\times q}$, $D_i \in \Re^{n\times l}$, $C_i \in \Re^{p\times n}$ are constant matrices of appropriate dimensions.

$\mu_i(\theta(t))$ are the weighting functions while respecting the properties of convex sets, as follows:

$$\mu_i(\theta(t)) > 0, \sum_{j=1}^{g} \mu_i(\theta(t)) = 1 \forall i \in [1, ...g] \tag{4}$$

$d(t)$ denotes the time-varying bounded state delay satisfying the following:

$$0 \le d(t) \le d_m, 0 \le \dot{d}(t) \le \tau < 1 \tag{5}$$

where d_m and τ are known constant scalars.

Recently, LPV systems with parameter-varying time delays have garnered significant interest due to their ability to model intricate systems characterized by nonlinearities and varying time delays. These systems present considerable challenges as they incorporate the complexities associated with both LPV and variable time-delay systems. One method to address these nonlinearities involves using local nonlinear models, which lead to a polytopic LPV representation with parameter-dependent variable time-delays.

This work is based on the following assumptions:

Assumption 1 ([5])**.** *Uncertainties and faults are assumed unknown. But they are bounded by some known constants. For the faults $f_a(t)$ and the uncertainties $\xi(x,t)$, there exist positive constants, such that we have the following:*

$$\|f_a(t)\| \le \rho_a \, , \|\xi(x,t)\| \le \beta \tag{6}$$

Assumption 2 ([5])**.** *The actuator fault repartition matrix $\mathcal{M}$ in (1) leads to the following:*

$$rank(C_i M_i) = q \tag{7}$$

Assumption 3 ([20])**.** *The system $\left(A_i + A_{di}e^{-ds}, M_i, C_i\right)$ has a relative degree of one and is minimum phase, characterized by the following:*

$$rank\left(\begin{bmatrix} sI_n - A_i - A_{di}e^{-ds} & M_i \\ C_i & 0_{p\times q} \end{bmatrix}\right) = n + q \tag{8}$$

holds for all complex numbers s where $\mathrm{Re}(s) \ge 0$*.*

A minimum-phase system guarantees stability even in the presence of actuator faults and uncertainties. It ensures that the non-asymptotically stable modes are observable (detectable).

Assumption 4 ([5])**.** *The known nonlinear function $\Gamma_i(x(t),t)$ satisfies a Lipschitz condition locally on a set $\mathbb{M} \subset \Re^n$ in which we have the following:*

$$\|\Gamma_i(x_1(t),t) - \Gamma_i(x_2(t),t)\| \le \gamma_1 \|x_1(t) - x_2(t)\| \tag{9}$$

$\forall x_1(t), x_2(t) \in \mathbb{M}$ *where γ_1 and γ_2 are unknown positives Lipschitz constants.*

In [27], the authors developed an SMO for the system, which can estimate stats and faults of a system respecting the following necessary assumptions, as recently used in [5]. Given the polytopic LPV delayed system (2) and (3), subject to actuator faults $f_a(t)$, uncertainties $\xi(t)$, and local nonlinearities $\Gamma_i(x(t),t)$, this paper presents a robust sliding mode control design based on sliding mode fault estimation. The primary objective is to address the following:

- Estimating the actuator fault and system states using adaptive sliding mode observers.
- Designing a sliding mode controller to stabilize the closed-loop system despite the occurrence of faults and uncertainties, while accounting for variable delay accuracy and nonlinearities.

Definition 1. *For matrices X and Y with appropriate dimensions, the following conditions apply:*

$$X^T Y + YX \le \delta^{-1} X^T X + \delta Y^T Y. \tag{10}$$

3. Robust Sliding Mode Fault Estimation Design

3.1. Transformation Coordinate System

Before presenting the main results of this paper, the objectives are twofold: to estimate actuator faults and system states using adaptive sliding mode observers, and to design a sliding mode controller that stabilizes the closed-loop system. This approach addresses the presence of faults and uncertainties, while also accounting for variable delay accuracy and local nonlinearities. Using Assumption 2, for the polytopic nonlinear LPV system with time delay (2) and (3), the following transformations exist [28]:

$$\begin{aligned} T_iA_iT_i^{-1} &= \begin{bmatrix} \bar{A}_{1i} & \bar{A}_{2i} \\ \bar{A}_{31i} & \bar{A}_{4i} \\ \bar{A}_{32i} & \end{bmatrix}, T_i\bar{A}_{di}T_i^{-1} = \begin{bmatrix} A_{d1i} & \bar{A}_{d2i} \\ \bar{A}_{d31i} & \bar{A}_{d4i} \\ \bar{A}_{d32i} & \end{bmatrix} \\ \bar{M}_{2i} &= \begin{bmatrix} 0 \\ \bar{M}_{qi} \end{bmatrix}, \bar{M}_i = \begin{bmatrix} 0 \\ \bar{M}_{2i} \end{bmatrix} \bar{C}_i = \begin{bmatrix} 0_{p\times(n_1-p)} & \bar{C}_{2i} \end{bmatrix}, \bar{D}_i = \begin{bmatrix} \bar{D}_{1i} \\ \bar{D}_{2i} \end{bmatrix} \end{aligned} \tag{11}$$

with $\tilde{M}_2i \in \Re^{p(q)}$, where $\tilde{C}_2i \in \Re^{p\times p}$ is nonsingular, with $p \geq q$.

The objective of this initial transformation is to create an efficient sliding mode observer capable of simultaneously estimating system states and actuator faults for the LPV system subject to local nonlinearities and time delays. This observer serves as the basis for the ensuing design of fault-tolerant control (FTC). Next, to identify the sliding mode, the second change of coordinates is as follows:

$$T_{Li} = \begin{bmatrix} I_{n-p} & L_i \\ 0 & \bar{C}_{2i} \end{bmatrix}, L_i = \begin{bmatrix} L_{1i} & 0_{(n-p)q} \end{bmatrix} \tag{12}$$

Consequently, the matrices (11) are transformed to be in the following forms:

$$\begin{aligned} T_{Li}\bar{A}_iT_{Li}^{-1} &= \begin{bmatrix} \tilde{A}_{1i} & \tilde{A}_{2i} \\ \tilde{A}_{31i} & \tilde{A}_{4i} \\ \tilde{A}_{32i} & \end{bmatrix}, T_{Li}\bar{A}_{di}T_{Li}^{-1} = \begin{bmatrix} \tilde{A}_{d1i} & \tilde{A}_{d2i} \\ \tilde{A}_{d31i} & \tilde{A}_{d4i} \\ \tilde{A}_{d32i} & \end{bmatrix} \\ \tilde{M}_i &= \begin{bmatrix} 0 \\ \tilde{M}_{2i} \end{bmatrix}, \tilde{M}_{2i} = \begin{bmatrix} 0 \\ \tilde{M}_{qi} \end{bmatrix} \tilde{D}_i = \begin{bmatrix} \tilde{D}_{1i} \\ \tilde{D}_{2i} \end{bmatrix}, \tilde{C}_i = \begin{bmatrix} 0_{p\times(n-p)} & I_p \end{bmatrix} \end{aligned} \tag{13}$$

with $\tilde{M}_2i \in \Re^{p(q)}$, where $\tilde{C}_2i \in \Re^{p\times p}$ is nonsingular, with $p \geq q$.

3.2. Sliding Mode Observer

By leveraging the universal approximation for uncertain nonlinear systems as presented in (13), this paper proposes a potential approach to developing a resilient polytopic adaptive SMO. This adaptive observer aims to enhance fault estimation, including actuator faults, in uncertain delayed systems. An adaptive observer for fault estimation is conceived to address the challenges associated with the following:

$$\begin{aligned} \dot{\hat{x}}(t) &= \sum_{j=1}^{g} \mu_i(\theta(t))\{\tilde{A}_i\hat{x}(t) + \tilde{A}_{di}\hat{x}(t-d(t)) + \Gamma_i(\tilde{x},t) \\ &+ \tilde{B}_iu(t) + \tilde{G}_{li}e_y(t) + \tilde{G}_{ni}v(t)\} \end{aligned} \tag{14}$$

$$\hat{y}(t) = \sum_{j=1}^{g} \mu_i(\theta(t))\{\tilde{C}_i\hat{x}(t)\} \tag{15}$$

with $\tilde{\Gamma}_i(x,t) = T_{Li}\begin{bmatrix} \Gamma_{1i}^T(x,t) & \Gamma_{2i}^T(x,t) \end{bmatrix}^T$. $\tilde{e}_y(t) = \hat{y}(t) - \tilde{y}(t)$ represents the output error estimation. The SMO gains $\tilde{G}_{ni}$ and $\tilde{G}_{li}$ are appropriately chosen gain matrices.

$$\tilde{G}_{ni} = \begin{bmatrix} -L_i\bar{C}_{2i}{}^T \\ \bar{C}_{2i}{}^T \end{bmatrix}, \tilde{G}_{li} = \begin{bmatrix} \tilde{G}_{l1i} \\ \tilde{G}_{l2i} \end{bmatrix} \tag{16}$$

with $L_i \in \Re^{(n-p)\times p} = \begin{bmatrix} L_{1,i} & 0_{(n-p)\times q} \end{bmatrix}$ defined in [16]. The robust adaptive sliding mode signal is expressed as follows:

$$v(t) = \begin{cases} -\rho(t)\frac{\bar{P}_2\,\bar{e}_y(t)}{\left\|\bar{P}_2\,\bar{e}_y(t)\right\|} & if\ \bar{e}_y(t) \neq 0 \\ 0 \quad otherwise \end{cases} \tag{17}$$

where $\bar{P}_2 \in \Re^{p\times p}$ is a positive definite symmetric matrix that will be found later and $\rho(t) = \hat{\rho} + \iota_0$ is a known positive scalar that limits the magnitude of the uncertainty and the fault signal. $\hat{\rho}$ is the adaptive update term defined by the following:

$$\dot{\hat{\rho}} = \vartheta\left\|\bar{P}_2\bar{e}_y(t)\right\|, \hat{\rho}(0) \geq 0 \tag{18}$$

Compared to the traditional sliding mode observer [29], the proposed adaptive sliding mode observer (14) and (15) is designed to address the challenge of abrupt variations in fault amplitude. This is accomplished by incorporating the adaptive update term (18), which improves the precision of both fault estimation and compensation. The adaptive term enables the observer to adapt to changes in fault characteristics, leading to more accurate fault estimates and better compensation capabilities. The adaptive mechanism enables the observer to adapt to changes in fault characteristics, allowing it to track sudden or unpredictable variations in fault magnitude. This feature is particularly beneficial in scenarios where the fault amplitude may change unexpectedly, as the adaptive approach allows the observer to provide reliable fault estimates for the fault-tolerant control. The new state estimation error is defined as $\dot{\tilde{e}}(t) = \dot{\hat{\tilde{x}}}(t) - \dot{\tilde{x}}(t)$ where we have the following:

$$\begin{aligned} \dot{\tilde{e}}(t) &= \sum_{j=1}^{g}\mu_i(\theta(t))\{(\tilde{A}_i - \tilde{G}_{li}\tilde{C}_i)\tilde{e}(t) + \tilde{\mathrm{A}}_{di}\tilde{e}(t-d(t)) - \tilde{D}\xi(x,t) + \tilde{\Gamma}_e(x,t) \\ &+ \tilde{G}_{ni}v(t) - \tilde{M}_i f_a(t)\} \end{aligned} \tag{19}$$

It is necessary to demonstrate the following:

$$\begin{aligned} \dot{\tilde{e}}_1(t) &= \sum_{j=1}^{g}\mu_i(\theta(t))\{\tilde{A}_{1i}\tilde{e}_1(t) + (\tilde{A}_{2i} - \tilde{G}_{l1i})\tilde{e}_1(t) + \tilde{\mathrm{A}}_{d1i}\tilde{e}_1(t-d(t)) + \tilde{\mathrm{A}}_{d2i}\tilde{e}_y(t-d(t)) \\ &+ \tilde{G}_{n1i}v(t) - \tilde{D}_{1i}\xi(x,t) + \tilde{\Gamma}_{e1i}(x,t)\} \end{aligned} \tag{20}$$

$$\begin{aligned} \dot{\tilde{e}}_y(t) &= \sum_{j=1}^{g}\mu_i(\theta(t))\{\tilde{A}_{3i}\tilde{e}_1(t) + (\tilde{A}_{4i} - \tilde{G}_{l2i})\tilde{e}_y(t)\tilde{\mathrm{A}}_{d3i}\tilde{e}_1(t-d(t)) + \tilde{\mathrm{A}}_{d4i}\tilde{e}_y(t-d(t)) \\ &- \tilde{D}_2\xi(x,t) + \tilde{\Gamma}_{e2i}(x,t) + \tilde{G}_{n2}v(t) - \tilde{M}_2 f_a(t)\} \end{aligned} \tag{21}$$

where $T_i\Gamma_e(x,t) = \begin{bmatrix} \tilde{\Gamma}_{e1i}(x,t) & \tilde{\Gamma}_{e2i}(x,t) \end{bmatrix}$.

This contribution aims to derive the matrix gains of the robust adaptive sliding mode observer (14) and (15) to estimate both actuator faults and state variables. This paper focuses on a polytopic LPV delayed system with local nonlinear models that satisfy the Lipschitz condition. It establishes sufficient conditions for the stability and H_∞ performance of the observer error using the Lyapunov–Krasovskii functional and multi-objective LMI technique. This paper begins by investigating the controlled estimation error $r(t)$ as a function of the system's input and output.

$$r(t) = H\begin{bmatrix} \dot{\tilde{e}}_1(t) \\ \dot{\tilde{e}}_2(t) \\ \dot{\tilde{e}}_1(t-d(t)) \\ \dot{\tilde{e}}_y(t-d(t)) \end{bmatrix} \tag{22}$$

Assume that H is a pre-specified weight matrix with full rank, i.e., $H = diag(H_1, H_2, H_3, H_4)$. We think about achieving the robust performance measure in its worst-case scenario, as follows:

$$\|H_\infty\| = \sup_{\|\xi\|_2 \neq 0} \frac{\|r(t)\|_2^2}{\|\xi(x,t)\|_2^2} \tag{23}$$

Now, we will introduce Theorem 1, outlining the necessary conditions for the existence of the suggested observer with a specified H_∞ performance $\|H_\infty\| < \sigma$.

Theorem 1. *Let us consider the LPV delayed system (2) and (3) under the verification of Assumptions (2) and (3). Provided these assumptions hold, the state estimation errors (20) and (21) exhibit asymptotic stability while achieving two objectives maximizing the admissible Lipschitz constant γ for the nonlinear function $\Gamma(x(t), t)$ and minimizing the gain σ for the system uncertainties $\xi(x, t)$. This scenario is possible given the existence of a fixed scalar value between 0 and 1 (represented as $0 \leq \lambda \leq 1$), positive constants ε, α, and σ, and specific matrices $P_1 > 0$, $P_2 > 0$, W_i. The fulfillment of these conditions hinges on the resolution of a convex multi-objective optimization problem in the form of an LMI.*

Minimize $[\lambda(\varepsilon + \alpha) + (1 - \lambda)\sigma]$ subject to the following:

$$\begin{bmatrix} \Pi_{1,i} & (P_1\tilde{A}_3)^T & P_1\tilde{A}_{d1} & P_1\tilde{A}_{d2} & P_1\tilde{D}_1 & P_1 & 0 & I_{n-p} & 0_{(n-p)p} \\ (*) & \Pi_{2,i} & P_2\tilde{A}_{d3} & P_2\tilde{A}_{d4} & P_2\tilde{D}_2 & 0 & P_2 & 0 & 0 \\ (*) & (*) & Z_1 & 0 & 0 & 0 & 0 & 0 & 0 \\ (*) & (*) & (*) & Z_2 & 0 & 0 & 0 & 0 & 0 \\ (*) & (*) & (*) & (*) & -\sigma I_l & 0 & 0 & 0 & 0 \\ (*) & (*) & (*) & (*) & (*) & -\varepsilon I_{n-p} & 0 & 0 & 0 \\ (*) & (*) & (*) & (*) & (*) & (*) & -\varepsilon I_p & 0 & 0 \\ (*) & (*) & (*) & (*) & (*) & (*) & (*) & -\alpha I_{n-p} & 0 \\ (*) & (*) & (*) & (*) & (*) & (*) & (*) & (*) & -\alpha I_p \end{bmatrix} < 0 \tag{24}$$

where

$\Pi_{1,i} = \bar{A}_{1i}^T P_1 + P_1\bar{A}_{1i} + W_i\bar{A}_{3i} + \bar{A}_{3i}^T W_i + S_1 + H_1^T H_1$,
$\Pi_{2,i} = \bar{A}_{4i}^{sT} P_2 + P_2\bar{A}_{4i}^s + S_2 + H_2^T H_2$
$Z_1 = -(1-\tau)S_1 + H_3^T H_3$, $Z_2 = -(1-\tau)S_2 + H_4^T H_4$

After solving the convex multi-objective problem, we demonstrate the following:

$$\begin{aligned} L_i &= P_1^{-1} W_i \\ \sigma^* &= \min(\sigma) \\ \alpha^* &= \min(\alpha) \\ \varepsilon^* &= \min(\varepsilon) \\ \gamma^* &= \min(\gamma) \end{aligned} \tag{25}$$

Proof. The proof of Theorem 1 is based on the Lyapunov–Krasovskii functional expressed by the following:

$$V(t) = V_1(t) + V_2(t) \tag{26}$$

where we have the following:

$$V_1(t) = \sum_{i=1}^{g} \mu_i(\theta(t)) \left\{ \tilde{e}_1^T(t) P_1 \tilde{e}_1(t) + \int_{t-d(t)}^{t} \tilde{e}_1^T(\theta) S_1 \tilde{e}_1(\theta) d\theta \right\}$$

and

$$V_y(t) = \sum_{i=1}^{g} \mu_i(\theta(t)) \left\{ \tilde{e}_y^T(t) P_2 \tilde{e}_y(t) + \int_{t-d(t)}^{t} \tilde{e}_y^T(\theta) S_2 \tilde{e}_y(\theta) d\theta \right\} .$$

where $P_1 \in \Re^{(n-p)\times(n-p)}$ and $P_2 \in \Re^{p\times p}$.

The time derivatives of $V_1(t)$ and $V_y(t)$ are managed in the following ways, respectively:

$$\begin{aligned} \dot{V}_1(t) &= \sum_{i=1}^{g} \mu_i(\theta(t)) \Big\{ \tilde{e}_1^T(t) \Psi_{1i} \tilde{e}_1(t) + 2\tilde{e}_1^T(t) P_1 \tilde{A}_{2i} \tilde{e}_y(t) + 2\tilde{e}_1^T(t) P_1 \tilde{A}_{1i} \tilde{e}_1(t-d(t)) \\ &- 2\tilde{e}_1^T(t) P_1 \tilde{D}_1 \xi(x,t) - (1-\tau) \tilde{e}_1^T(t-d(t)) S_1 \tilde{e}_1(t-d(t)) \\ &+ 2\tilde{e}_1^T(t) P_1 T_{Li} \Big(\Gamma_{e1i}\Big(T_{Li}^{-1} x, t\Big) - \Gamma_{e1i}\Big(T_{Li}^{-1} \hat{x}, t\Big) \Big) \Big\} \end{aligned} \tag{27}$$

and

$$\begin{aligned} \dot{V}_y(t) &= \sum_{i=1}^{g} \mu_i(\theta(t)) \Big\{ \tilde{e}_y^T(t) \Psi_{2i} \tilde{e}_y(t) + 2\tilde{e}_y^T(t) P_2 \tilde{A}_{d3i} \tilde{e}_1(t-d(t)) + 2\tilde{e}_y^T(t) P_2 \tilde{A}_3 \tilde{e}_1(t) \\ &+ 2\tilde{e}_y^T(t) P_2 \tilde{A}_{d4i} \tilde{e}_1(t-d(t)) + 2\tilde{e}_y^T(t) P_2 \left(\tilde{M}_{2i} f(t) - v(t) - \frac{1}{\beta} \dot{\tilde{\rho}} \rho \right) \\ &+ 2\tilde{e}_y^T(t) P_2 T_{Li} \Big(\Gamma_{e2i}\Big(T_{Li}^{-1} x, t\Big) - \Gamma_{e2i}\Big(T_{Li}^{-1} \hat{x}, t\Big) \Big) \\ &- 2\tilde{e}_y^T(t) P_2 \tilde{D}_2 \xi(x,t) + 2\tilde{e}_1^T(t) P_1 \tilde{A}_{d2i} \tilde{e}_y(t-d(t)) \\ &- (1-\tau) \tilde{e}_y^T(t-d(t)) S_2 \tilde{e}_y(t-d(t)) \Big\} \end{aligned} \tag{28}$$

with $\Psi_{1i} = \tilde{A}_{1i}^T P_1 + P_1 \tilde{A}_{1i} + W_i \tilde{A}_{3i} + \tilde{A}_{3i}^T W_i + S_1$, $\Psi_{2i} = \tilde{A}_{4i}^{sT} P_2 + P_2 \tilde{A}_{4i}^s + S_2$.

Applying Definition 1 and considering Assumption 4, we demonstrate that the known nonlinear function $\Gamma_{e1i}\Big(T_{Li}^{-1} x, t\Big)$ is designed as follows:

$$\begin{aligned} & 2\tilde{e}_1^T(t) P_1 T_{Li} \Big(\Gamma_{e1i}\Big(T_{Li}^{-1} x, t\Big) - \Gamma_{e1i}\Big(T_{Li}^{-1} \hat{x}, t\Big) \Big) \\ & \leq \tfrac{1}{\varepsilon} \tilde{e}_1^T(t)\, P_1{}^2 \tilde{e}_1(t) + \varepsilon \Big[\Gamma_{e1i}\Big(T_{Li}^{-1} x, t\Big) - \Gamma_{e1i}\Big(T_{Li}^{-1} \hat{x}, t\Big) \Big]^T \\ & \times T_{Li}^T T_{Li} \Big[\Gamma_{e1i}\Big(T_{Li}^{-1} x, t\Big) - \Gamma_{e1i}\Big(T_{Li}^{-1} \hat{x}, t\Big) \Big] \\ & = \tfrac{1}{\varepsilon} \tilde{e}_1^T(t)\, P_1{}^2 \tilde{e}_1(t) + \varepsilon \Big\| T_{Li} \Big[\Gamma_{e1i}\Big(T_{Li}^{-1} x, t\Big) - \Gamma_{e1i}\Big(T_{Li}^{-1} \hat{x}, t\Big) \Big] \Big\|^2 \\ & \leq \tfrac{1}{\varepsilon} \tilde{e}_1^T(t)\, P_1{}^2 \tilde{e}_1(t) + \varepsilon \gamma^2 \|T_{Li}\|^2 \|\tilde{e}_1(t)\|^2 \\ & \leq \tfrac{1}{\varepsilon} \tilde{e}_1^T(t) P_1{}^2 \tilde{e}_1(t) + \varepsilon \tilde{\gamma}^2 \|\tilde{e}_1(t)\|^2 \end{aligned} \tag{29}$$

where γ is the Lipschitz constant of $\Gamma_{e1i}\Big(T_{Li}^{-1} x, t\Big)$ and $\tilde{\gamma} = \gamma \|T_{Li}\|$. Likewise, for the known nonlinear function $\Gamma_{e2i}\Big(T_{Li}^{-1} x, t\Big)$, the following inequality can be readily expressed as follows:

$$2\tilde{e}_y^T(t) P_2 T_{Li} \Big(\Gamma_{e2i}\Big(T_{Li}^{-1} x, t\Big) - \Gamma_{e2i}\Big(T_{Li}^{-1} \hat{x}, t\Big) \Big) \leq \frac{1}{\varepsilon} \tilde{e}_y^T(t) P_2{}^2 \tilde{e}_y(t) + \varepsilon \tilde{\gamma}^2 \|\tilde{e}_y(t)\|^2 \tag{30}$$

On the other hand, considering the definition of $v(t)$ in (17) and the bound on $\|f_a(t)\| < \rho_a$, we can derive the following inequality:

$$\begin{aligned}&2\tilde{e}_y^T(t)P_2\left(\tilde{M}_{2i}f(t)-v(t)-\tfrac{1}{\beta}\dot{\hat{\rho}}\rho\right)\leq \tilde{e}_y^T(t)\tilde{M}_{2i}^TP_2\|f_a(t)\|\\&-\rho(t)\tilde{e}_y^T(t)P_2\tfrac{P_2\tilde{e}_y(t)}{\|P_2\tilde{e}_y(t)\|}-(\rho-\hat{\rho})\|P_2\tilde{e}_y(t)\|\\&\leq \tilde{e}_y^T(t)\tilde{M}_{2i}^TP_2\|f_a(t)\|-(\hat{\rho}+v)\left\|\tilde{e}_y^T(t)P_2\right\|-(\rho-\hat{\rho})\|P_2\tilde{e}_y(t)\|\\&\leq v_{i,\max}\|P_2\tilde{e}_y(t)\|-v\|P_2\tilde{e}_y(t)\|<0\end{aligned} \tag{31}$$

where $v_{i,\max}=\|\tilde{M}_{2i}\|_{\max}\rho_a$ with $v_{i,\max}\leq\rho_a$.

Now, using (30) and (31), we can write the following:

$$\begin{aligned}&\dot{V}(t)\leq\sum_{j=1}^{g}\mu_i(\theta(t))\Big\{\tilde{e}_1^T(t)\left(\Psi_{1i}+\tfrac{1}{\varepsilon}+\varepsilon\tilde{\gamma}^2I_{n-p}\right)\tilde{e}_1(t)\\&+2\tilde{e}_1^T(t)P_1\tilde{A}_{1i}\tilde{e}_1(t-d(t))+2\tilde{e}_1^T(t)P_1\tilde{A}_{2i}\tilde{e}_y(t)\\&-(1-\tau)\tilde{e}_1^T(t-d(t))S_1\tilde{e}_1(t-d(t))\\&+\tilde{e}_y^T(t)\left(\Psi_{2i}+\tfrac{1}{\varepsilon}+\varepsilon\tilde{\gamma}^2I_p\right)\tilde{e}_y(t)\\&-2\tilde{e}_y^T(t)P_2\tilde{D}_2\xi(x,t)+2\tilde{e}_1^T(t)P_1\tilde{A}_{d2i}\tilde{e}_y(t-d(t))\\&+2\tilde{e}_y^T(t)P_2\tilde{A}_{d3i}\tilde{e}_1(t-d(t))+2\tilde{e}_y^T(t)P_2\tilde{A}_3\tilde{e}_1(t)\\&+2\tilde{e}_y^T(t)P_2\tilde{A}_{d4i}\tilde{e}_1(t-d(t))-2\tilde{e}_1^T(t)P_1\tilde{D}_1\xi(x,t)\\&-(1-\tau)\tilde{e}_y^T(t-d(t))S_2\tilde{e}_y(t-d(t))\Big\}\end{aligned} \tag{32}$$

To ensure the resilience of the proposed adaptive SMO to the uncertainties $\xi(x,t)$ in the L_2 sense, we introduce the subsequent variable V_0 as follows:

$$V_0=V(t)+r^T(t)r(t)-\sigma\xi^T(x,t)\xi(x,t)<0 \tag{33}$$

We introduce the new variable as follows:

$$\alpha=\frac{1}{\varepsilon\tilde{\gamma}^2}\rightarrow\tilde{\gamma}=\frac{1}{\sqrt{\alpha\varepsilon}} \tag{34}$$

The maximization of $\tilde{\gamma}$ for the Lipschitz nonlinear function $\bar{\Gamma}_i(x,t)$ can be achieved by concurrently minimizing both α and ε. By integrating these two objective functions, our goal is to minimize the linear function as follows: $\alpha+\varepsilon$

$$V_0(t)\leq\sum_{i=1}^{g}\mu_i(\theta(t))\begin{bmatrix}\tilde{e}_1^T(t)\\\tilde{e}_y^T(t)\\\tilde{e}_1^T(t-d(t))\\\tilde{e}_y^T(t-d(t))\\\xi^T(x,t)\end{bmatrix}^T\Theta_i\begin{bmatrix}\tilde{e}_1(t)\\\tilde{e}_y(t)\\\tilde{e}_1(t-d(t))\\\tilde{e}_y(t-d(t))\\\xi(x,t)\end{bmatrix} \tag{35}$$

with

$$\Theta_i=\begin{bmatrix}\Theta_{1,i}&\left(\tilde{A}_3P_1\right)^T&P\tilde{A}_{d1}&P\tilde{D}\\(*)&\Theta_{2,i}&0&0\\(*)&(*)&Z&0\\(*)&(*)&(*)&\sigma I_l\end{bmatrix}$$

where

$$\Theta_{1,i}=\tilde{A}_{1i}^TP_1+P_1\tilde{A}_{1i}+W_i\tilde{A}_{3i}+\tilde{A}_{3i}^TW_i+S_1+\tfrac{1}{\varepsilon}P_1{}^2+\varepsilon\tilde{\gamma}^2I_{n-p}+H_1^TH_1 \text{ and}$$
$$\Theta_{2,i}=\tilde{A}_{4i}^{sT}P_2+P_2\tilde{A}_{4i}^s+S_2+\tfrac{1}{\varepsilon}P_2{}^2+\varepsilon\tilde{\gamma}^2I_p+H_2^TH_2.$$

$$Z=\begin{bmatrix}-(1-\tau)S_1+H_3^TH_3&0\\0&-(1-\tau)S_2+H_4^TH_4\end{bmatrix}.$$

Therefore, $V_0(t) \leq 0$ if:

$$\sum_{i=1}^{g} \mu_i(\theta(t))\Theta_i < 0 \tag{36}$$

According to the Shur compliment, we can obtain (24) using (36). Furthermore, if (24) is achieved, then we conclude that $V(t) = V_1(t) + V_2(t) < 0$. It remains to verify that state estimation errors (20) and (21) are asymptotically stable with an attenuation level $\|H_\infty\| \leq \sigma$. This completes the proof. □

3.3. Robust Fault Estimation

In this section, it is assumed that the adaptive sliding mode observer defined by Equations (14) and (15) has been constructed, and the reachability condition $S_g(t)$ is met. Consequently, we have the following:

$$S_g(t) = \{(\tilde{e}_1(t), \tilde{e}_y(t)) | \tilde{e}_y(t) = 0\} \tag{37}$$

On the sliding surface $S_g(t)$, the state estimation error remains stable $\sup\limits_{0 \leq t \leq \infty} \|\tilde{e}_1(t)\| \leq \varpi$ where ϖ is a positive scalar. The objective of sliding motion reachability is to ensure that the system's state trajectories reach and maintain motion along a predetermined sliding surface $S_g(t)$. This involves designing a control strategy that drives the system's state toward the sliding surface and ensures it remains on this surface for subsequent times, despite the presence of local nonlinearities and variable time delays. We assume that the given positive constants κ_0 and $\rho(t)$ meet the following inequality:

$$\rho(t) \geq \kappa_{\max} + \kappa_0 \tag{38}$$

Then, the error dynamics (20) and (21) can be set to the sliding surface $S_g(t)$ given by (37). This implies the following: $\dot{e}_y(t) = e_y(t) = 0$. So, in order to obtain a robust fault estimation, the following structure is used:

$$\begin{aligned} \dot{\tilde{e}}_y \quad &= \quad 0 = \sum_{j=1}^{g} \mu_i(\theta(t))\{\tilde{A}_{3i}\tilde{e}_1(t) + \tilde{A}_{d3i}\tilde{e}_1(t - d(t)) + \tilde{\Gamma}_{e2i}(x,t) + \tilde{G}_{n2}v_{eq}(t) \\ &- \quad \tilde{D}_2\xi(x,t) - \tilde{M}_2 f_a(t)\} \end{aligned} \tag{39}$$

Here, $v_{eq}(t)$ represents the equivalent output error injection signal required to sustain the sliding motion. This signal can be approximated to any desired level of accuracy by substituting (17) with the following:

$$v_{eq}(t) = \rho(t)\frac{P_2 e_y}{\|P_2 e_y\| + \delta} \tag{40}$$

where δ is a small positive scalar to reduce the chattering effect.

We derive the following relationship:

$$\Omega(\tilde{e}_1, x, t) = \sum_{j=1}^{g} \mu_i(\theta(t))\{\tilde{A}_{3i}\tilde{e}_1(t) + \tilde{A}_{d3i}\tilde{e}_1(t - d(t)) + \tilde{\Gamma}_{e2i}(x,t) - \tilde{D}_2\xi(x,t)\} \tag{41}$$

We have the following:

$$\|\Omega(\tilde{e}_1, x, t)\|_2 \leq \sum_{j=1}^{g} \mu_i(\theta(t))\kappa_{\max} \tag{42}$$

where $\kappa_{\max} = (\|\tilde{A}_{3i}\|_2 + \|\tilde{A}_{d3i}\|_2 + \gamma)\varpi + \|\tilde{D}_2\|_2\beta$.

From the last equation, we can conclude the following:

$$\|\Omega(\tilde{e}_1, x, t)\| \leq \kappa_{\max} \tag{43}$$

For a sufficiently small value of the maximum fault magnitude $\kappa_{\max}$, the following can be inferred:

$$0 = \sum_{i=1}^{g} \mu_i(\theta(t))\big(\tilde{M}_{2i} f_a(t) - v_{eq}(t)\big) \tag{44}$$

The estimation of actuator faults will be obtained based on the equivalent error injection signal, and it is expressed by the following expressions:

$$\hat{f}_a(t) = \sum_{i=1}^{g} \mu_i(\theta(t))\big(\tilde{M}_{2i}\big)^{+}\left\{\frac{\bar{P}_0\ \bar{e}_y(t)}{\|\bar{P}_0\ \bar{e}_y(t)\| + \delta}\right\} \tag{45}$$

A design procedure for fault estimation based on an adaptive SMO is introduced in a revised version, as follows:

Step 1: Choose the weight matrix predefined in Equation (22).
Step 2: Choose a suitable scalar $0 \leq \lambda \leq 1$; we can obtain the matrices P_1; P_2; W_i and the scalars ε, ς, and γ by resolving the LMI optimization problem (24) using the MATLAB (2015b) LMI toolbox.
Step 3: Actuator fault estimation can be achieved via an adaptive SMO design (14) and (15) and using Equations (39) and (45).

The next section explores a fault-tolerant control design for the uncertain nonlinear delay system through the information supplied by the estimation of actuator faults.

4. Sliding Mode Controller Design

The intended sliding mode controller with an adaptive law is designated to take corrective actions to counteract fault influences and stabilize the nonlinear system characterized by LPV-delayed representation.

The main objective of this work is to create an effective and resilient fault-tolerant control (FTC) strategy for specific types of uncertain systems that include local nonlinear models and variable time-delays. This approach introduces a sliding mode FTC technique based on fault estimation (FE) to address the complexities of such systems. The significant contributions of this study include the following:

- The designs for FE and FTC are specifically developed to handle variable time-delays in the polytopic system, presenting greater challenges compared to systems with constant time delays.
- The sliding mode control method is utilized to ensure robustness against uncertainties and disturbances, making the proposed strategy ideal for applications dealing with high levels of uncertainty or nonlinearity in polytopic systems.

Let us define a sliding surface S_g as follows:

$$S_g := \{y(t) \in \Re^p : S_c(t) = 0\} \tag{46}$$

$S_c(t) \in {}^m$ a linear switching function based on output feedback information for nonlinear systems could be described as follows:

$$S_c(t) = \sum_{i=1}^{g} \mu_i(\theta(t))\{N_{c,i} y(t)\} \tag{47}$$

with $N_{c,i} = (C_i B_i)^{+} - h\Big(I_p - C_i B_i (C_i B_i)^{+}\Big)$ with an arbitrary matrix $h \in {}^{m \times p}$ and $(C_i B_i)^{+} = \Big((C_i B_i)^{+}(C_i B_i)\Big)^{1}(C_i B_i)^{T}$.

Prior to initiating the fault-tolerant control (FTC) design, given the assumption that the pair (A_i, B_i) is controllable, and using the estimation of actuator faults and the system state, we suggest formulating a robust control as follows:

$$u(t) = u_l(t) + u_n(t) \tag{48}$$

The control input $u_l(t)$ is designed to incorporate the linear component, which is influenced by the system states and the estimation of actuator faults, as specified by the following:

$$u_l(t) = \sum_{j=1}^{g} \mu_i(\theta(t)) \left\{ -k_j \hat{x}(t) - q_i \hat{f}_a(t) \right\} \tag{49}$$

where $q_i \hat{f}_a(t)$ aims to mitigate the impact of actuator faults. It is presupposed that $k_j \in \Re^{m \times n}$ and $q_i = B_i M_i$.

Real-time adjustments of the K_j gains and fault estimation $\hat{f}_a(t)$ are facilitated by adaptive algorithms. Real-time control heavily relies on feedback mechanisms, where the current state of the system informs adjustments to control gains, thanks to the adaptive nature of our SMC. The nonlinear $u_n(t)$ component responsible for initiating the sliding motion on the surface, S_g, is introduced with an adaptive law as follows:

$$u_n(t) := \begin{cases} \eta(t) \frac{S_c(t)}{\|S_c(t)\|} & if\ S_c(t) = 0 \\ 0 & otherwise \end{cases} \tag{50}$$

$\eta(t) = \hat{\rho}_c + \iota_c + \varpi_c$ where $\iota_c > 0$ and $\varpi_c > 0$ is positive small constants. We use $\hat{\rho}_c$ to determine the term $\eta(t)$.

We note the following:

$$\dot{\hat{\rho}}_c S_c = \varpi_c \|S_c(t)\|, \hat{\rho}_c(0) \geq 0 \tag{51}$$

where ϖ_c is a positive gain.

According to the preceding information, utilizing the distinct adaptive nonlinear component structure of $u_n(t)$, it is necessary to demonstrate that the system will inevitably converge to and remain on the associated sliding mode surface S_g within a finite time. Consequently, when examining the sliding motion corresponding to the sliding surface S_g outlined in (46), we contemplate the Lyapunov–Krasovskii function as our analytical tool.

$$V_c(t) = \frac{1}{2} S_c^T(t) S_c(t) + \frac{1}{2\varpi_c} \tilde{\rho}_c^2 \tag{52}$$

where $\tilde{\rho}_c = \rho_c - \hat{\rho}_c$ is the estimated error of ρ_c.

This optimal Lyapunov function not only guarantees stability but also minimizes the effect that results in chattering, thereby improving system performance despite the presence of local nonlinearities, uncertainties, and variable time-delay. Our study addresses this challenge by incorporating adaptive mechanisms into the design of the Lyapunov function to enhance both robustness and optimality. Referring to the dynamic equations of the open-loop system in (2) and (47), the time derivative of (52) yields the following:

$$\dot{V}_c(t) = \sum_{i=1}^{g} \sum_{j=1}^{g} \mu_i \mu_j(\theta(t)) \left\{ \left(N_{c,i} C_i A_i - k_j \right) \|x(t)\| \, N_{c,i} C_i A_{di} \|x(t - d(t))\| - \iota_c - \varpi_c \right\} \|S_c(t)\| \} \tag{53}$$

We define the subassembly system with the following expression:

$$\Omega_c = \{ x \|x(t)\| \leq \kappa_c \} \tag{54}$$

The condition for reachability, ensuring the system reaches the sliding surface S, is met when the scalar ι_c is chosen to satisfy $\iota_c > \left(N_{c,i}C_iA_i - k_j\right)\kappa_c$ such that we have the following:

$$S^T{}_c(t)S_c(t) \leq -\varpi_c\|S_c(t)\| \tag{55}$$

The suggested sliding mode controller with adaptive law guarantees the presence of an optimal sliding motion within a finite duration; specifically, $\dot{S}_c(t)S_c(t) = 0$, $\forall t \geq t_c$. Upon achieving the sliding mode, our attention turns toward assessing the stability of the closed-loop delayed LPV system utilizing local nonlinear models. Let us introduce the equivalent control u_{eq}:

$$\begin{aligned} u_{eq} &= \sum_{i=1}^{g} \mu_j(\theta(t))\{N_{c,i}C_i\{[A_ix(t) + A_{di}x(t-d(t)) \\ &+ \Gamma(x,t) + D_i(x,t)]\} + u_l(t) \end{aligned} \tag{56}$$

The closed-loop system's dynamics incorporating the equivalent control law (56) are represented as follows:

$$\begin{aligned} \dot{X}(t) &= \sum_{i=1}^{g}\sum_{j=1}^{g} \mu_i\mu_j(\theta(t))\{\theta_i\left(A_i - k_{1j}B_i\right)x(t) \\ &+ \theta_iA_{di}x(t-d(t)) + \theta_i\Gamma(x,t) + B_{ij}E(t)\} \end{aligned} \tag{57}$$

$$y_c(t) = \sum_{i=1}^{g} \mu_i(\theta(t))\{C_ix(t)\} \tag{58}$$

with $B_{ij} = \begin{bmatrix} Bk_{1j} & M_i & \theta_iD_i \end{bmatrix}$, $E_i(t) = \begin{bmatrix} e_x^T(t) & e_{f_a}^T(t) & \xi^T(x,t) \end{bmatrix}^T$ and $\theta_i = I_n - B_iN_{c,i}C_i$.

The nonlinear function $\Gamma(x,t)$ satisfies a Lipschitz condition in (9); the following assumption is also required:

$$\|\Gamma(x,t)\| = \gamma\|x(t)\| \tag{59}$$

where $\gamma > 0$ is Lipschitz-constant.

The Lipschitz condition is used to ensure that the controller can effectively overcome uncertainty without leading to instability. It is used to design control laws that ensure that the system can reach the sliding surface and stay there despite variable time-delays and uncertainty.

The current objective is to establish the necessary conditions for ensuring the stability of the closed-loop LPV delayed system (57) and (58) on the sliding surface S_g in the presence of actuator faults, uncertainties, and time delays simultaneously.

5. Fault-Tolerant Control Design

Thus, we propose designing an FTC strategy aimed at providing corrective action after the detection of faults and disturbances, as well as stabilizing the system. Two cases are considered, depending on the characteristics of the delays, so that we have the following:

- Separated design FTC with variable time-delay.
- Integrated design and FTC with variable time-delay.

5.1. Separated Fault-Tolerant Control Design

Over the past years, significant research efforts have been dedicated to addressing the fault estimation (FE)-based fault-tolerant control (FTC) problem in a precise and effective manner. Previous studies have primarily focused on tackling this issue through a two-step approach or separated approach:

Step 1: Develop an observer to estimate the faults and system states.
Step 2: Design a controller to stabilize the closed-loop system.

The conventional approach to the FE-based FTC design for uncertain polytopic systems with local nonlinear models and variable time-delays can be depicted as separated architecture, as shown in Figure 1.

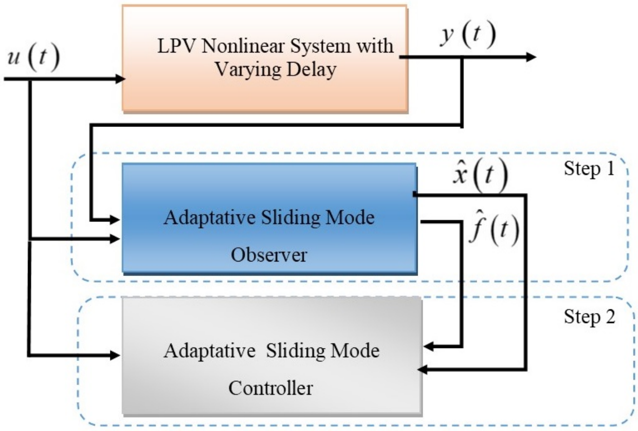

Figure 1. Separated Design FTC.

The following theorem provides sufficient conditions for the existence of such an FTC control, with prescribed H_∞ performances, by using Lyapunov–Krasovskii stability and the multi-objective LMI technique.

Theorem 2. *The closed loop for a nonlinear delayed system is robustly stable with the simultaneously maximized admissible Lipschitz constant λ_x and minimized gain ς_x. The H_∞ criteria are guaranteed if there exists a symmetric positive definite matrix $P_x = P_x^T$, Q, and constants $0 \leq \lambda_x \leq 1$, $\alpha_x > 0$ and $\varsigma_x > 0$, such that the following LMI optimization holds:*

$$\begin{array}{l} min[\lambda_x(\varepsilon_x + \alpha_x) + (1-\lambda_x)\varsigma_x] \\ \begin{bmatrix} \Psi_{i,j} + C_i^T C_i & \theta_i A_{di} & B_i Q_j & E_i \\ * & (1-\tau)S_x & 0 & 0 \\ * & * & -2\vartheta + \varsigma_x I_n & 0 \\ * & * & * & \mathrm{N} \end{bmatrix} < 0 \end{array} \tag{60}$$

where $\Psi_{i,j} = P_x A_i^T \theta_i{}^T + \theta_i A_i P_x - B_i Q_j - B_i^T Q_j^T + S_{xi}$, $\vartheta = \mu_c P_x$ *and* $K_j = Q_j P_x{}^{-1}$,
$\bar{E}_i = \begin{bmatrix} M_i & \theta_i D_i & P_x C_i^T & P_x & I_n \\ 0 & 0 & 0 & 0 & 0 \end{bmatrix}$, *and* $\mathrm{N} = diag\{-\varsigma_x I_n, -\varsigma_x I_q, -\varsigma_x I_l, -I, -\varepsilon_x I, -\alpha_x I\}$.

Upon resolving the multi-objective optimization problem, the following is demonstrated:

$$\begin{array}{rcl} \varsigma_x^* & = & \min(\varsigma_x) \\ \alpha_x^* & = & \min(\alpha_x) \\ \varepsilon_x^* & = & \min(\varepsilon_x) \\ \lambda_x^* & = & \min(\lambda_x) \end{array} \tag{61}$$

Proof. Let us introduce the Lyapunov function for the closed-loop system as follows:

$$V_x(t) = x^T(t) P_x x(t) + \int_{t-d(t)}^{t} x^T(t) S_x x(t) dx \tag{62}$$

where $P_x \in \Re^{n \times n}$ is a symmetric positive definite matrix. By considering the closed-loop LPV delayed system (57) and (58), the time derivative $\dot{V}_x(t)$ can be addressed as follows:

$$\begin{aligned}\dot{V}_x(t) &= \sum_{i=1}^{g}\sum_{i=1}^{g}\mu_i\mu_j(\theta(t))\Big\{x^T(t)\Pi_{xi}x(t) + 2x^T(t)P_x\theta_iA_{di}x(t) + 2x^T(t)P_x\theta_i\Gamma(x,t)\\ &- x^T(t-d(t))(1-\tau)S_xx(t-d(t)) - 2x^T(t)P_xB_iE_i(t)\Big\}\end{aligned} \tag{63}$$

with $\Pi_{xi} = P_x\theta_i{}^TA_i{}^T + \theta_iA_iP_x - Q_j{}^TB_ij^T - B_ijQ_j + S_{xi}$.

Based on the definition and Assumption 4, the following inequality is derived:

$$\begin{aligned}&2x^T(t)P_x\theta_i\Gamma(x,t) \le \tfrac{1}{\varepsilon_c}x^T(t)P_xx(t) + \varepsilon_c\Gamma^T(x,t)\theta^T{}_i\theta_i\Gamma(x,t)\\ &\le x^T(t)\left[\tfrac{1}{\varepsilon_c}P_x^2 + \varepsilon_c\tilde{\gamma}_c^2\right]x(t)\end{aligned} \tag{64}$$

We note the following: $\tilde{\gamma}_c = \gamma_c\|\theta_i\|$.

To guarantee the resilience of the closed-loop LPV delayed system (57) and (58) against disturbances denoted by $\phi(t)$, we introduce the variable $J(t)$ defined as follows:

$$J(t) = \sum_{i=1}^{g}\sum_{i=1}^{g}\mu_i\mu_j(\theta(t))\{\dot{V}_x(t) + Y_L^T(t)Y_L(t) - \varsigma_x\phi^T(t)\phi(t)\} \tag{65}$$

We can rewrite the above expression as follows:

$$\begin{aligned}J(t) &= \sum_{i=1}^{g}\sum_{i=1}^{g}\mu_i\mu_j(\theta(t))\Big\{x^T(t)\Big(\Pi_{xi} + C_i^TC_i\Big)x(t) + 2x^T(t)P_{xi}\theta_iA_{di}x(t)\\ &+ x^T(t)\left[\frac{1}{\varepsilon_c}P_x^2 + \varepsilon_c\tilde{\gamma}_c^2\right]x(t) + 2x^T(t)P_xB_iE_i(t)\Big\} < 0\end{aligned} \tag{66}$$

We introduce the new variable as follows:

$$\alpha_c := \frac{1}{\varepsilon_c\tilde{\gamma}_c^2} \to \tilde{\gamma}_c = \frac{1}{\sqrt{\varepsilon_c\tilde{\gamma}_c}} \tag{67}$$

It has been determined that maximizing $\tilde{\gamma}_c$, associated with the nonlinear Lipschitz function $\Gamma(x,t)$, can be achieved by concurrently minimizing both ε_c and α_c, implying the need to minimize the linear function $\alpha_c + \varepsilon_c$. Therefore, the following remains to be shown:

$$\Sigma_{sep} = \sum_{i=1}^{g}\sum_{i=1}^{g}\mu_i\mu_j(\theta(t))\begin{bmatrix}\Lambda_{1,ij} & \Lambda_{2ij}\\ (*) & \Lambda_{3ij}\end{bmatrix} < 0 \tag{68}$$

with $\Lambda_{1,ij} = \begin{bmatrix}\Pi_{xi,j} & \theta_iA_{di}\\ * & (1-\tau)S_x\end{bmatrix}$, $\Lambda_{2,ij} = \begin{bmatrix}P_xM_i & P_x\theta_iD_i & P_xC_i^T & P_x & I_n\\ 0 & 0 & 0 & 0 & 0\end{bmatrix}$,
$\Lambda_{3ij} = diag\{-\varsigma_xI_n, -\varsigma_xI_q, -\varsigma_xI_l, -I, -\varepsilon_xI, -\alpha_xI\}$.

Based on the Schur complement, the relationship (68) is equivalent to the following:

$$\sum_{i=1}^{g}\sum_{i=1}^{g}\mu_i\mu_j(\theta(t))\begin{bmatrix}\Pi_{xi,j} & \theta_iA_{di} & P_xB_ik_j & P_xM_i & P_x\theta_iD_i & P_xC_i^T & P_x & I_n\\ * & (1-\tau)S_x & 0 & 0 & 0 & 0 & 0 & 0\\ * & * & -\varsigma_xI_n & 0 & 0 & 0 & 0 & 0\\ * & * & * & -\varsigma_xI_q & 0 & 0 & 0 & 0\\ * & * & * & * & -\varsigma_xI_l & 0 & 0 & 0\\ * & * & * & * & * & -I & 0 & 0\\ * & * & * & * & * & * & -\alpha_xI & 0\\ * & * & * & * & * & * & * & -\varepsilon_xI\end{bmatrix} < 0 \tag{69}$$

with $\Pi_{xi,j} = P_xA_i{}^T + A_iP_x - Q_j{}^TB_i{}^T - B_iQ_j + S_x$ and $P_x = P_x{}^{-1}$.

Next, we will construct the matrix X with a unique diagonal structure as follows: $X = diag\{P_x^{-1}, P_x^{-1}, P_x^{-1}, I_q, I_l, I_p, I_n, I_n\}$. By multiplying both sides of Equation (60) by X and its transpose, we arrive at Equation (63). Using the definition, we can then establish the following relationship:

$$P_x{}^{-1} + P_x{}^{-1} \leq \varsigma_x P_x{}^{-1} P_x{}^{-1} + \varsigma_x{}^{-1} I_n \tag{70}$$

It is evident that Equation (70) is equivalent to the following:

$$P_x{}^{-1} \varsigma_x P_x{}^{-1} \leq -2P_x{}^{-1} + \varsigma_x{}^{-1} I_n \tag{71}$$

Through the use of the previous results, it is straightforward to deduce that the closed-loop LPV delayed system (57) and (58) with local nonlinear models is robustly stable with respect to the H_∞ performance level ς_x and the maximized admissible Lipschitz constant γ_c.

This completes the proof. □

An adaptive separated FTC design procedure using an adaptive SMO is described as follows:

Step 1: Choose a suitable scalar "$0 \leq \lambda_x \leq 1$"; resolve the LMI optimization problem (60) using the MATLAB (2015b) LMI toolbox. We can now obtain the matrix Q_j and the scalars δ_x, ς_x, and γ_x.
Step 2: Calculate $K_j = Q_j \bar{P}_x^{-1}$.
Step 3: Construct the adaptive SMC (50); thus, the closed-loop nonlinear system stability (Equations (57) and (58)) can be achieved.

5.2. Integrated Fault-Tolerant Control Design

In recent years, several studies have been published on the design of fault-tolerant control (FTC) systems using finite element (FE) methods, which involve a single step to achieve optimal robustness between observer and controller models as shown in Figure 2.

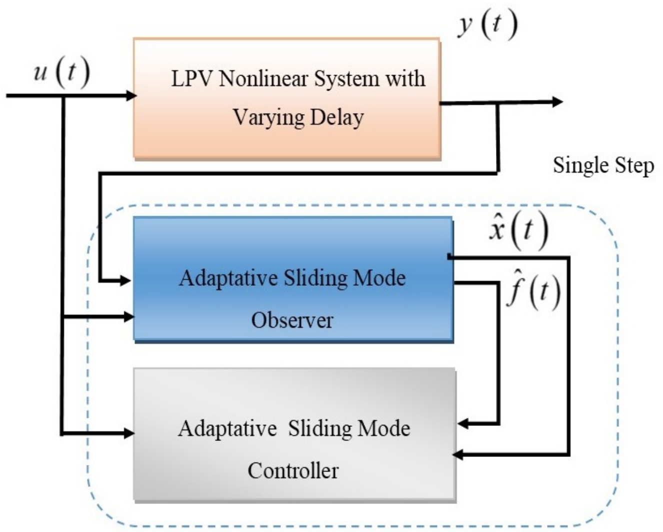

Figure 2. Integrated design of FTC.

In this section, we investigate the potential of the integrated FE-based FTC design to compute, in a single step, adaptive observer gains G_{li} and controller gains K_j. This approach aims to enhance the robustness of the closed-loop nonlinear system despite the presence of time-delay nonlinearities and uncertainties. Combining (20), (21), (57), and (58) yields the following delayed closed-loop system, including fault estimation with fault compensation control, expressed as follows:

$$\begin{aligned} \dot{X}(t) &= \sum_{i=1}^{g} \sum_{j=1}^{g} \mu_i \mu_j(\theta(t)) \{\theta_i (A_i - k_{1j} B_i) x(t) + \theta_i A_{di} x(t - d(t)) \\ &+ \theta_i \Gamma(x,t) + B_{ij} E(t)\} \end{aligned} \tag{72}$$

$$\begin{aligned}
\dot{\tilde{e}}_1(t) &= \sum_{j=1}^{g} \mu_i(\theta(t))\{\tilde{A}_{1i}\tilde{e}_1(t) + (\tilde{A}_{2i} - \tilde{G}_{l1i})\tilde{e}_1(t) + \tilde{G}_{n1i}v(t) \\
&+ \tilde{\mathrm{A}}_{d1i}\tilde{e}_1(t-d(t)) + \tilde{\mathrm{A}}_{d2i}\tilde{e}_y(t-d(t)) - \tilde{D}_{1i}\xi(x,t) \\
&+ \tilde{\Gamma}_{e1i}(x,t)\} \qquad (73)\\
\dot{\tilde{e}}_y(t) &= \sum_{j=1}^{g} \mu_i(\theta(t))\{\tilde{A}_{3i}\tilde{e}_1(t) + (\tilde{A}_{4i} - \tilde{G}_{l2i})\tilde{e}_y(t) - \tilde{D}_2\xi(x,t) \\
&+ \tilde{\mathrm{A}}_{d3i}\tilde{e}_1(t-d(t)) + \tilde{\mathrm{A}}_{d4i}\tilde{e}_y(t-d(t)) + \tilde{\Gamma}_{e2i}(x,t) \\
&+ \tilde{G}_{n2}v(t) + \tilde{\mathrm{A}}_{d4i}\tilde{e}_y(t-d(t)) - \tilde{M}_2 f_a(t)\} \qquad (74)\\
Y_{\mathrm{int}}(t) &= \sum_{i=1}^{g} \mu_i(\theta(t))\{C_{L_i}x(t) + C_{Li}e(t)\} \qquad (75)
\end{aligned}$$

with $B_{ij} = \begin{bmatrix} Bk_{1j} & M_i & \theta_i D_i \end{bmatrix}$, $E_i(t) = \begin{bmatrix} e_x^T(t) & e_{f_a}^T(t) & \xi^T(x,t) \end{bmatrix}^T$ and $\theta_i = I_n - B_i N_{c,i} C_i$. The boundlessness of $e_x(t)$ and $e_{f_a}(t)$ can be guaranteed based on Theorem 2; based on Assumption 4, the following theorem is presented to design feedback gain matrices $k_j \in \Re^{p\times n}$ ensuring that the closed-loop LPV delayed nonlinear system (72)–(75) remains stable.

Theorem 3. *Using the sliding mode input structure (47), the closed-loop LPV delayed system, as represented by Equations (72)–(75), achieves robust stability with an optimized admissible Lipschitz constant $\gamma_i > 0$ and minimized gain $\|H_{\mathrm{int}}\|_\infty < \varsigma_c$. This is contingent on the existence of constants $0 \le \lambda_x \le 1$ and $\alpha_i > 0$, and matrices $P_x = P_x^T > 0$, $P_e = P_e^T > 0$, $S_e > 0$, YY, and Q_j such that the following LMI optimization is verified:*

$$\begin{gathered}
min[\lambda_e(\varepsilon_e + \alpha_e) + (1-\lambda_c)\varsigma_c] \\
\begin{bmatrix}
\chi_{11} & \chi_{12} & \chi_{13} & \chi_{14} & \chi_{15} & \chi_{16} \\
* & \chi_{21} & \chi_{22} & \chi_{23} & \chi_{24} & \chi_{25} \\
* & * & \chi_{31} & \chi_{32} & \chi_{33} & \chi_{34} \\
* & * & * & \chi_{41} & \chi_{42} & \chi_{43} \\
* & * & * & * & \chi_{51} & \chi_{52} \\
* & * & * & * & * & \chi_{61}
\end{bmatrix} < 0
\end{gathered} \qquad (76)$$

We note the following:

$$\begin{aligned}
\chi_{11} &= \Pi_{xi} + \frac{1}{\varepsilon_i}P_e^2 + \varepsilon_i\tilde{\gamma}^2 I_n, \chi_{12} = (\theta_i A_{di})^T \\
\chi_{15} &= P_x B_{i,j}\chi_{16} = P_x C_L^T C_L, \chi_{21} = -(1-\tau)S_x \\
\chi_{13} &= \chi_{14} = \chi_{22} = \chi_{25} = \chi_{32} = \chi_{33} = \chi_{34} = 0 \\
\chi_{23} &= P_e\tilde{A}_{di}, \chi_{24} = P_e\bar{\bar{D}}_i, \chi_{31} = \Pi_i + \frac{1}{\varepsilon}P_e{}^2 + \varepsilon\tilde{\gamma}^2 I_{n-p} \\
\chi_{41} &= -(1-\tau)S_e, \chi_{42} = \chi_{43} = 0 \\
\chi_{51} &= -2Y + \varsigma_c I, \chi_{52} = 0, \chi_{61} = -I_n \\
\Pi_i &= \begin{bmatrix} \Pi_{1,i} & (P_1\tilde{A}_{3i})^T \\ * & \Pi_{2,i} \end{bmatrix}, \bar{\bar{D}}_i = \begin{bmatrix} 0 & \tilde{M}_i & \tilde{D}_i \end{bmatrix} \\
\Pi_{xi} &= P_x\theta_i{}^T A_i{}^T + \theta_i A_i P_x - Q_j{}^T B_i{}^T - B_i Q_j + S_{xi} \\
\Pi_{1i} &= \tilde{A}_{1i}^T P_1 + P_1\tilde{A}_{1i} + W_i\tilde{A}_{3i} + \tilde{A}_{3i}^T W_i + S_1 + \frac{1}{\varepsilon}P_1 + \varepsilon\tilde{\gamma}^2 I_{n-p} + H_1^T H_1 \qquad (77)\\
\Pi_{2i} &= \tilde{A}_{4i}^{sT} P_2 + P_2\tilde{A}_{4i}^s + S_2 + \frac{1}{\varepsilon}P_2 + \varepsilon\tilde{\gamma}^2 I_p + H_2^T H_2
\end{aligned}$$

where $P_e = diag\{P_1, P_2\}$ and $S_e = diag\{S_1, S_2\}$ are symmetric definite positive matrices.

The gain matrices of the adaptive sliding mode controller K_j and observer $G_{L,i}$ are computed as follows:

$$K_j = Q_j {P_x}^{-1} \tag{78}$$
$$G_{L,i} = P_1 W_{1,i} \tag{79}$$

Proof. To ensure the stability of the LPV-delayed nonlinear system, as described by Equations (72)–(75), we construct a Lyapunov–Krasovskii functional as follows:

$$V_{\text{int}}(t) = V_x(t) + V(t) \tag{80}$$

We assume the following:

$$V_x(t) = x^T(t)P_x x(t) + \int_{t-d(t)}^{t} x^T(t)S_x x(t)dx \tag{81}$$

$$V(t) = e^T(t)P_e e(t) + \int_{t-d(t)}^{t} e^T(t)S_e e(t)dx \tag{82}$$

We can follow a similar approach to Theorems 1 and 2 and consider the closed-loop LPV delayed system. Therefore, the time derivative of $V_{\text{int}}(t)$ is given by the following:

$$\begin{aligned}
&\dot{V}_{\text{int}}(t) = \sum_{i=1}^{g}\sum_{i=1}^{g} \mu_i\mu_j(\theta(t))\Big\{x^T(t)\Big(\Pi_{xi} + \tfrac{1}{\varepsilon_i}I_n + \varepsilon_i\tilde{\gamma}^2 I_n\Big)x(t) \\
&+2x^T(t)P_x(\theta_i A_{di})^T x(t-d(t)) - 2x^T(t)P_x B_{i,j}E_i(t) \\
&-x^T(t-d(t))(1-\tau)S_x x(t-d(t)) \\
&+\tilde{e}^T(t)P_e\begin{bmatrix} \Lambda_{1,i} & 0 \\ 0 & \Lambda_{2,i}\end{bmatrix}\tilde{e}(t) + \tfrac{1}{\varepsilon_i}\tilde{e}^T(t){P_e}^2 + \varepsilon_i\gamma^2\tilde{e}^T(t)^T \\
&+2\tilde{e}^T(t)P_e\tilde{A}_i\tilde{e}^T(t-d(t)) + 2\tilde{e}^T(t)P_e\tilde{A}_{di}\tilde{e}^T(t-d(t)) \\
&+2\tilde{e}^T(t)P_e\tilde{D}_i\zeta(x,t) + 2\tilde{e}^T(t)P_e\left(\begin{bmatrix} 0 \\ \tilde{M}_{2i}\end{bmatrix}f(t) - v(t)\right) \\
&+\tilde{e}^T(t)S_e\tilde{e}(t) - (1-\tau)\tilde{e}^T(t-d(t))S_e\tilde{e}(t-d(t))\}
\end{aligned} \tag{83}$$

Let us consider the term $J(t)$ as follows:

$$J(t) = \sum_{i=1}^{g}\sum_{i=1}^{g} \mu_i\mu_j(\theta(t))\Big\{\dot{V}_{\text{int}}(t) + Y_L^T(t)Y_L(t) - \varsigma_c {E_i}^T(t)E_i(t)\Big\} \tag{84}$$

We can rewrite the last expression as follows:

$$\begin{aligned}
&J(t) = \sum_{i=1}^{g}\sum_{i=1}^{g} \mu_i\mu_j(\theta(t))\{x^T(t)\big(\Lambda_{x,ij} + C_L^T C_L\big)x(t) + 2x^T(t)P_x(\theta_i A_{di})^T x(t-d(t)) \\
&-2x^T(t)P_x B_{i,j}E_i(t) - x^T(t-d(t))(1-\tau)S_x x(t-d(t)) \\
&+\tilde{e}^T(t)P_e\begin{bmatrix} \Lambda_{1,i} & 0 \\ 0 & \Lambda_{2,i}\end{bmatrix}\tilde{e}(t) + \tfrac{1}{\varepsilon_i}\tilde{e}^T(t){P_e}^2 + \varepsilon_i\gamma^2\tilde{e}^T(t) \\
&+2\tilde{e}^T(t)P_e\tilde{A}_i\tilde{e}^T(t-d(t)) + 2\tilde{e}^T(t)P_e\tilde{A}_{di}\tilde{e}^T(t-d(t)) \\
&+\tilde{e}^T(t)S_e\tilde{e}(t) - (1-\tau)\tilde{e}^T(t-d(t))S_e\tilde{e}(t-d(t)) \\
&+2\tilde{e}^T(t)P_e\bar{\bar{D}}_i E_i(t) + \tilde{e}^T(t)\big(C_e^T C_e\big)\tilde{e}(t) - \varsigma_c {E_i}^T(t)E_i(t)\Big\}
\end{aligned} \tag{85}$$

We note that $\bar{\bar{D}}_i = \begin{bmatrix} 0 & \tilde{M}_i & \tilde{D}_i \end{bmatrix}$.
Equivalently, in matrix form, the expression can be written as follows:

$$J(t) \le \sum_{i=1}^{g}\sum_{i=1}^{g} \mu_i\mu_j(\theta(t))\Big\{\Xi^T(t)\Psi_{ij}\Xi(t)\Big\} \tag{86}$$

where $\Xi(t) = \begin{bmatrix} x^T(t) & x^T(t-d(t)) & \tilde{e}^T(t) & \tilde{e}^T(t-d(t)) & E_i(t) \end{bmatrix}^T$.

We define Ψ_{ij} as follows:

$$\Psi_{ij} = \sum_{i=1}^{g}\sum_{i=1}^{g}\mu_i\mu_j(\theta(t))\begin{bmatrix} \Lambda_{xi} & (\theta_i A_{di})^T & 0 & 0 & B_{i,j} \\ * & -(1-\tau)S_x & \Lambda_i + \frac{1}{\varepsilon_i}P_e{}^2 I_n + \varepsilon_i\gamma^2 I_n & P_e\tilde{A}_{di} & P_e\bar{D}_i \\ * & * & * & -(1-\tau)S_e & 0 \\ * & * & * & * & 0 \\ * & * & * & * & \varsigma_c I \end{bmatrix} \tag{87}$$

Thus, $P_e = diag(P_1, P_2)$ and $S_e = diag(S_1, S_2)$ with the following:

$$\begin{aligned} \Lambda_i &= diag(\Lambda_{1,i}, \Lambda_{2,i}) \\ \Lambda_{1,i} &= \tilde{A}_{1i}^T P_1 + P_1\tilde{A}_{1i} + W_i\tilde{A}_{3i} + \tilde{A}_{3i}^T W_i + S_1 + H_1^T H_1 + \frac{1}{\varepsilon}P_1{}^2 + \varepsilon\tilde{\gamma}^2 I_{n-p} \\ \Lambda_{2,i} &= \tilde{A}_{4i}^T P_2 - W_{2,i}^T + P_2\tilde{A}_{4i} - W_{2i} + S_2 + \frac{1}{\varepsilon}P_2{}^2 + \varepsilon\tilde{\gamma}^2 I_p + H_2^T H_2 \\ \Lambda_{xi} &= P_x A_i^T \theta_i{}^T + \theta_i A_i P_x - B_i Q_j - B_i^T Q_j^T + S_{xi} + C_L^T C_L + \frac{1}{\varepsilon_i} I_n + \varepsilon_i\tilde{\gamma}^2 I_n \end{aligned}$$

To achieve the required transformation, we construct matrix X with a unique diagonal structure, as $X = \left\{P_x{}^{-1}, P_x{}^{-1}, I_n, I_n, P_x{}^{-1}\right\}$. By pre- and post-multiplying X and its transpose in Ψ_{ij}, applying Lemma 1, and performing straightforward manipulations, it is clear that (87) is equivalent to (76). From this, we can conclude that the augmented closed-loop LPV delayed system subject to nonlinearities, described by Equations (72)–(75), is robustly stable against $e_x(t)$, $e_f(t)$, $\xi(x,t)$ with respect to the H_∞ performance level.

This completes the proof. □

An adaptive integrated FTC design procedure using an adaptive SMO is described as follows:

Step 1: Choose a suitable scalar "$0 \le \lambda_x \le 1$"; resolve the LMI optimization problem (60) using the MATLAB (2015b) LMI toolbox. We can then obtain the matrix Q_j and the scalars δ_c, ς_c and γ_c.
Step 2: Calculate $K_j = Q_j\bar{P}_x^{-1}$.
Step 3: Construct the adaptive SMC (50); thus, the closed-loop nonlinear system stability (72)–(75) can be produced.

6. Illustrative Example

In this section, the design of both separated and integrated sliding mode FTC strategies is carried out, utilizing the data provided by the sliding mode observer. The LPV model of the diesel engine, obtained from [30], is considered for this purpose (see Figure 3). Diesel engines are designed to resist severe operating conditions, making them suitable for environments where uncertainty can affect the system. Integrating diesel engines into variable time-delay LPV systems enables better management of the delays inherent in engine operation. The mean value of the diesel engine model is obtained by providing the mass and energy and the ideal gas law. The time delays and nonlinearity present in the diesel engine dynamics can have a destabilizing effect and degrade closed-loop performance.

In state space, it is described as follows:

$$x(t) = \begin{bmatrix} x_1(t) : Intake\ manifold\ pressure \\ x_2(t) : Exhaust\ manifold\ pressure \\ x_3(t) : Compressor\ power \end{bmatrix}$$

and the inputs are as follows:

$$u(t) = \begin{bmatrix} u_1(t) : Control\ input\ for\ valve\ pening \\ u_2(t) : Control\ input\ for\ the\ turbine \end{bmatrix}$$

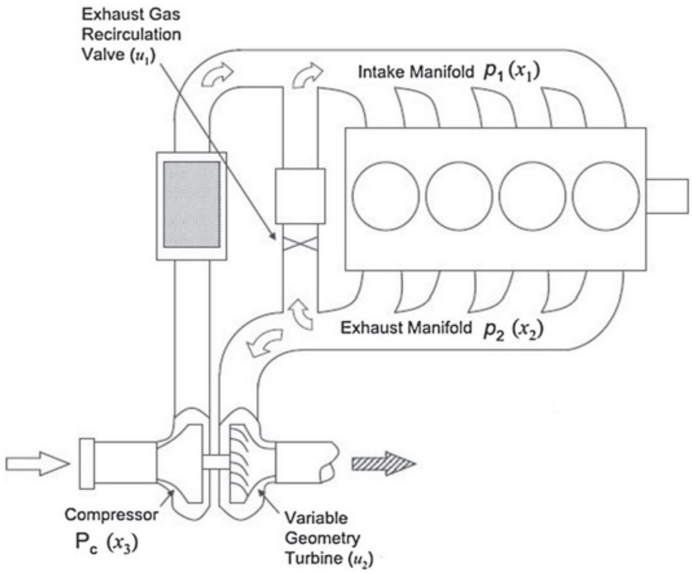

Figure 3. The air path system of diesel engines.

6.1. LPV System with Variable Time-Delay

Let us first consider the nonlinear model of the diesel engine system without any faults and nonlinearity, which can be expressed as follows:

$$\begin{aligned} \dot{x}(t) &= \varphi_{x1}(x(t)) + \varphi_{x2}(x(t))x(t-d(t)) + \varphi_{x3}(x(t))u(t) + \varphi_{x4}(x(t))\xi(x,t) \\ y(t) &= \varphi_2(x(t)) \\ y_L(t) &= \varphi_{yl}(x(t)) \end{aligned} \tag{88}$$

Then, we express the LPV local nonlinear model subject to the actuator fault, uncertainty, and variable time-delay in the following form:

$$\begin{aligned} \dot{x}(t) &= \sum_{i=1}^{4} \mu_i(\theta(t))\{A_i(t)x(t) + A_{di}(t-d(t)) \\ &+ D_i\xi(t,x) + B_iu(t) + \Gamma_i(x,u) + M_if_a(t) \\ y(t) &= \sum_{i=1}^{4} \mu_i(\theta(t))\{C_ix(t)\} \end{aligned} \tag{89}$$

The weighting functions $\mu_i(\theta(t))$ are defined as follows:

$$\begin{aligned} \mu_1(\theta(t)) &= \frac{(\theta_1(t)+0.6)(\theta_2(t)+2)}{4} \\ \mu_2(\theta(t)) &= \frac{(\theta_1(t)+0.6)(2-\theta_2(t))}{4} \\ \mu_3(\theta(t)) &= \frac{(0.6-\theta_1(t))(\theta_2(t)+2)}{4} \\ \mu_4(\theta(t)) &= \frac{(0.6-\theta_1(t))(2-\theta_2(t))}{4} \end{aligned} \tag{90}$$

with $\theta_1(t) = 0.25\sin(0.1t)$, $\theta_2(t) = 0.1\sin(0.25t)$.

The proposed approach encapsulates the nonlinearities present in the diesel engine system, allowing for effective handling of the nonlinear dynamics:

$$\Gamma(x,t) = \begin{bmatrix} -3.33\sin(x_3(t)) \\ 0 \\ 0 \end{bmatrix} \tag{91}$$

Based on the convex set of the LPV system (89), the matrices of local nonlinear models in (90) can be expressed as follows:

$$\begin{aligned}
A_1 &= \begin{bmatrix} -12.6 & 4.6 & 0 \\ 0.41 & -2.08 & 0 \\ 0.486 & -0.0004 & -1.33 \end{bmatrix}, A_2 = \begin{bmatrix} -12.6 & 4.6 & 0 \\ 0.41 & -2.08 & 0 \\ 0.486 & -0.4404 & -1.33 \end{bmatrix} \\
A_3 &= \begin{bmatrix} -12.6 & 4.6 & 0 \\ 1.62 & -2.08 & 0 \\ 0.726 & -0.4404 & -1.33 \end{bmatrix}, A_4 = \begin{bmatrix} -12.6 & 4.6 & 0 \\ 1.62 & -2.08 & 0 \\ 0.726 & -0.0004 & -1.33 \end{bmatrix} \\
A_{d1} &= A_{d2} = A_{d3} = A_{d4} = \begin{bmatrix} 0 & 3.6 & 0 \\ 0 & 0 & 0 \\ 0 & 0 & 0 \end{bmatrix} \\
B_1 &= B_2 = B_3 = B_4 = \begin{bmatrix} 0 & 0 \\ -25.65 & 40.32 \\ -18.27 & 1 \end{bmatrix}, C_1 = C_2 = C_3 = C_4 = \begin{bmatrix} 1 & 0 & 0 \\ 1 & 0 & 1 \end{bmatrix}, \\
D_1 &= D_2 = D_3 = D_4 = 0.1 \times \begin{bmatrix} 1 \\ 0.91 \\ 0.91 \end{bmatrix}, M_1 = M_2 = M_3 = M_4 = \begin{bmatrix} 0.7 \\ 0 \\ 1 \end{bmatrix}
\end{aligned} \tag{92}$$

The delay is modeled as a variable time-delay: $d(t) = 0.1\sin(0.3t)$.

Let us assume that an actuator fault occurs in the input channel of the diesel engine system. This fault will be added to the state equation, which can be described as follows:

$$f_a(t) = \begin{cases} 0 & 0 \leq t < 4s \\ \sin(t) & 4 \leq t < 15s \end{cases} \tag{93}$$

For the nonlinear LPV delayed system, comparative simulations are provided to evaluate the performance of the separated and integrated fault estimation (FE)-based fault-tolerant control (FTC) designs. The same system parameters and initial conditions are used for both the separated and integrated FE-based FTC approaches to enable a fair comparison.

6.2. Separated FTC Design

Obviously, Assumptions 2 and 3 are verified based on the matrices of the nonlinear models, that is, $rank(CM) = rank(M) = 1$, $\left(A_i + A_{di}e^{-ds}, M, C\right)$ is a minimum phase $n \geq p = 2$ and $q = 1$. The adaptive sliding mode observer method presented in the following can be used for the nonlinear diesel engine system to achieve robust actuator fault estimation. Based on the information provided by the observer, an adaptive sliding mode controller will be designed in order to stabilize the diesel engine system. The design parameters were chosen as follows: $\lambda = 0.1, H_1 = H_3 = I_{n-p}, H_2 = 2I_p, H_4 = I_p$ and $\tilde{A}^s_{22} = diag(-10, -7)$. Using the MATLAB LMI Toolbox, we can solve Theorem 1 and design an adaptive observer (14) and (15).

$$
\begin{aligned}
G_{l1} &= \begin{bmatrix} 2.420 & 1.388 \\ 9.054 & 1.484 \\ -9.156 & 5.669 \end{bmatrix} G_{n1} = \begin{bmatrix} 1 & 0 \\ 1.09 & 0.30 \\ -1 & 1 \end{bmatrix} \\
G_{l2} &= \begin{bmatrix} 2.864 & 1.032 \\ 9.819 & 1.104 \\ -9.679 & 5.571 \end{bmatrix} G_{n2} = \begin{bmatrix} 1 & 0 \\ 1.18 & 0.22 \\ -1 & 1 \end{bmatrix} \\
G_{l3} &= \begin{bmatrix} 2.839 & 1.045 \\ 10.97 & 1.118 \\ -8.464 & 5.569 \end{bmatrix} G_{n3} = \begin{bmatrix} 0.437 & 0.009 \\ 1.182 & 0.22 \\ -1 & 1 \end{bmatrix} \\
G_{l4} &= \begin{bmatrix} 2.227 & 1.494 \\ 9.92 & 1.598 \\ -7.944 & 5.669 \end{bmatrix} G_{n4} = \begin{bmatrix} 1 & 0 \\ 1.049 & 0.32 \\ -1 & 1 \end{bmatrix}
\end{aligned} \tag{94}
$$

and we find the following:

$$
P_e = \begin{bmatrix} 1.912 & 0 & 0 \\ 0 & 1.456 & -0.324 \\ 0 & -0.324 & 1.027 \end{bmatrix} \tag{95}
$$

Based on Theorem 2, the sliding mode controller gains can be described as follows:

$$
\begin{aligned}
k_1 &= \begin{bmatrix} -13.09 & -4.98 & -2.98 \\ 9.54 & 7.17 & 2.11 \end{bmatrix}, k_2 = \begin{bmatrix} -12.94 & -4.92 & -2.97 \\ 9.64 & 7.15 & 2.10 \end{bmatrix} \\
k_3 &= \begin{bmatrix} -12.92 & -5.02 & -2.98 \\ 9.75 & 7.10 & 2.10 \end{bmatrix}, k_4 = \begin{bmatrix} -12.76 & -5.06 & -2.97 \\ 10.10 & 7.19 & 2.15 \end{bmatrix}
\end{aligned} \tag{96}
$$

and

$$
P_x = \begin{bmatrix} 7.61 & 1.05 & 1.20 \\ 1.05 & 3.86 & 0.71 \\ 1.20 & 0.71 & 0.41 \end{bmatrix} \tag{97}
$$

6.3. Integrated FTC Design

By solving the LMI conditions presented in Theorem 3 using the "mincx" function of the MATLAB LMI Toolbox, we can compute the matrix gains of the adaptive observer (as defined in Equations (14) and (15)) and the sliding mode controller (as defined in Equation (48)) in a single step, as follows:

$$
\begin{aligned}
G_{l1} &= \begin{bmatrix} 14.79 & -2.01 \\ 30.67 & -2.15 \\ -9.15 & 5.67 \end{bmatrix} G_{n1} = \begin{bmatrix} 1 & 0 \\ 3.82 & -0.43 \\ -1 & 1 \end{bmatrix} \\
G_{l2} &= \begin{bmatrix} 13.74 & -2.91 \\ 28.54 & -3.11 \\ -10.72 & 5.94 \end{bmatrix} G_{n2} = \begin{bmatrix} 1 & 0 \\ 3.55 & -0.33 \\ -1 & 1 \end{bmatrix} \\
G_{l3} &= \begin{bmatrix} 13.80 & -2.65 \\ 29.85 & -2.84 \\ -9.51 & 5.62 \end{bmatrix} G_{n3} = \begin{bmatrix} 1 & 0 \\ 3.56 & -0.57 \\ -1 & 1 \end{bmatrix} \\
G_{l4} &= \begin{bmatrix} 13.76 & -2.40 \\ 29.79 & -2.56 \\ -9. & 5.67 \end{bmatrix} G_{n4} = \begin{bmatrix} 1 & 0 \\ 3.55 & -0.52 \\ -1 & 1 \end{bmatrix}
\end{aligned} \tag{98}
$$

and

$$\begin{aligned} P_e &= \begin{bmatrix} 4.51 & 0 & 0 \\ 0 & 11.19 & -1.18 \\ 0 & -1.182 & 1.51 \end{bmatrix}, P_x = \begin{bmatrix} 7.61 & 1.05 & 1.20 \\ 1.05 & 3.86 & 0.71 \\ 1.20 & 0.71 & 0.41 \end{bmatrix} \\ k_1 &= k_3 = \begin{bmatrix} -78.83 & -59.76 & -189.05 \\ 2.78 & 9.667 & -36.97 \end{bmatrix}, \\ k_2 &= \begin{bmatrix} -78.72 & -59.60 & -188.79 \\ -3.22 & 9.05 & -38.00 \end{bmatrix}, k_4 = \begin{bmatrix} -78.71 & -59.60 & -188.78 \\ -3.21 & 9.07 & -37.79 \end{bmatrix} \end{aligned} \tag{99}$$

Furthermore, the optimized LMI gains for the integrated and separated fault estimation (FE)-based fault-tolerant control (FTC) designs are listed in Table 1. As can be observed, the level of uncertainty attenuation, which relates to the integrated approach, is significantly lower compared to the separated approach. The separated approach loses a certain degree of robustness against uncertainties, which illustrates the improvement in fault estimation and compensation achieved through the integrated FTC approach.

Table 1. LMI optimization gains.

	Integrated FTC	**Separated FTC**
Uncertainty attenuation level	$\varsigma_c = 4.47$	$\varsigma_x = 13.47$
Admissible Lipschitz constant	$\gamma_c = 0.014$	$\gamma_x = 37.47$

We have learned that the nonlinear function satisfies the Lipschitz condition. Consequently, the admissible Lipschitz constant, which relates to the integrated approach, is higher than the one provided by the separated approach, thus illustrating the superiority of the integrated FE-based FTC approach in handling a broader range of nonlinear functions. The simulation results demonstrate the effectiveness of the proposed approach, which includes online actuator fault estimation and compensation for the closed-loop nonlinear system in the presence of uncertainties $\xi(x,t) = 0.1(0.3\sin(t) + 0.5x_1(t))$.

The results are presented as follows:

$$\begin{aligned} \rho_1 &= \rho_2 = \rho_3 = \rho_4 = 10 \\ \delta_1 &= \delta_2 = \delta_3 = \delta_4 = 0.01 \\ \tau &= 0.3, \bar{\omega} = 1.1 \end{aligned} \tag{100}$$

The sliding mode signal, as defined in Equation (17), is designed with the goal of $\eta(t) = \hat{\rho} + 15$, such that the adaptive update term is defined as $\dot{\hat{\rho}} = 1.1\|P_2 e_y(t)\|$.

The sliding mode controller (48) is considered, where we have the following: $N_{c,1} = N_{c,2} = N_{c,3} = N_{c,4} = \begin{bmatrix} -0.3 & 0 \\ 0 & 1 \end{bmatrix}$. The initial conditions are as follows: $x_1(0) = x_2(0) = x_3(0) = x_4(0) = \begin{bmatrix} 0.02 \\ -0.03 \\ -0.05 \end{bmatrix}$.

The simulation results demonstrate the effectiveness of the proposed approach, which includes online actuator fault estimation and compensation. Figure 4 illustrates the actuator fault estimation, showcasing the ability of the proposed adaptive sliding mode observer (defined by Equations (14) and (15)) to estimate actuator faults with satisfactory precision while rejecting the effects of system uncertainties and variable time-delays.

As illustrated in Figure 4, it is important to note that despite the presence of uncertainties and variable time-delays, the proposed sliding mode observer with the adaptive equivalent injection can track the actuator fault $f_a(t)$ more accurately compared to the traditional observer without the adaptive law. This demonstrates the effectiveness of the adaptive sliding mode observer in handling challenging system characteristics, such as uncertainties and time-varying delays, and providing improved fault estimation performance.

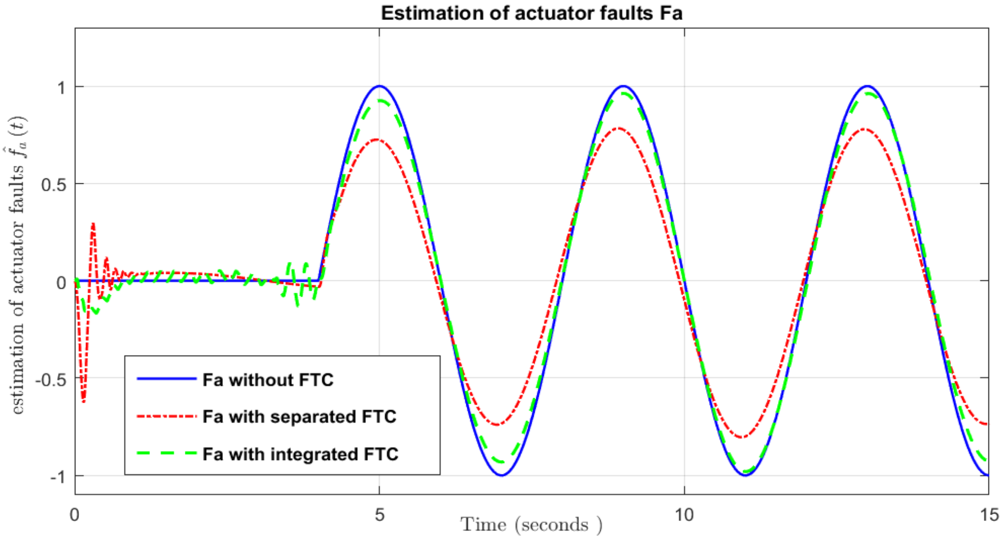

Figure 4. Estimation of actuator fault: Actuator fault estimation without FTC (blue line), actuator fault estimation with the separated FTC (red line), and actuator fault estimation with the integrated FTC (green line).

The comparative study of the time-domain response of the closed-loop system outputs between the integrated sliding mode FTC and the separated sliding mode FTC is shown in Figures 5 and 6. We can conclude that the proposed controllers stabilize the closed-loop system when the system is affected by nonlinearity, actuator faults, and variable time-delays. Thus, the performances are guaranteed while compensating for the effect of the faults. Furthermore, in Figures 7 and 8 through to the integrated sliding mode FTC, the system can quickly reach stability compared to the separated approach. The integrated FTC based on SMC can smooth the control law, ensuring a high response rate to stabilize the system (first response at $t = 0.05$ s).

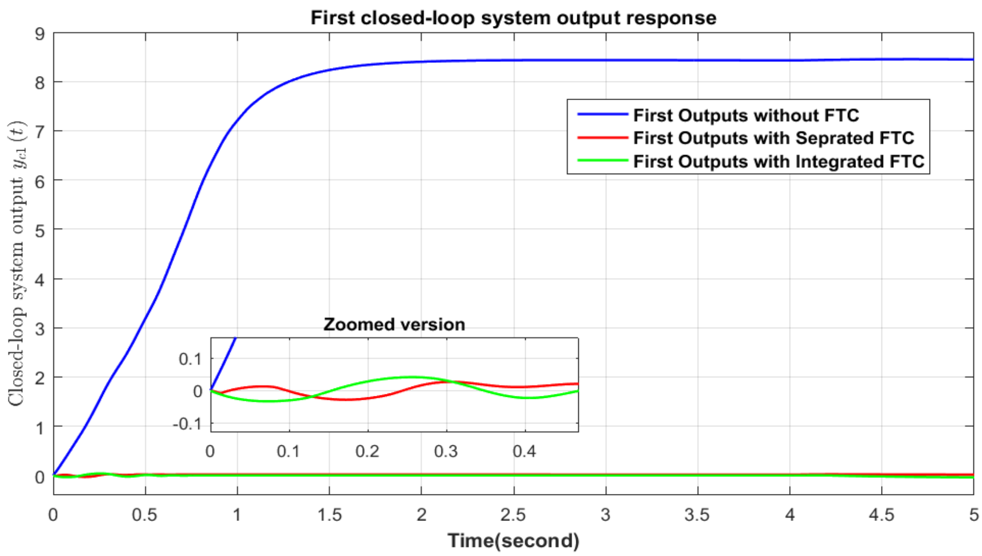

Figure 5. First closed-loop system output response: output response with the separated FTC (red line) and output response with the integrated FTC (green line).

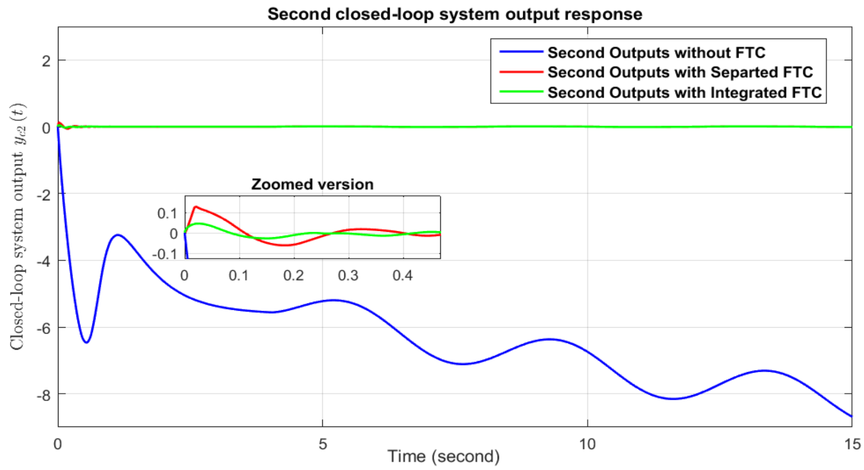

Figure 6. Second closed-loop system output response: output response with the separated FTC (red line) and output response with the integrated FTC (green line).

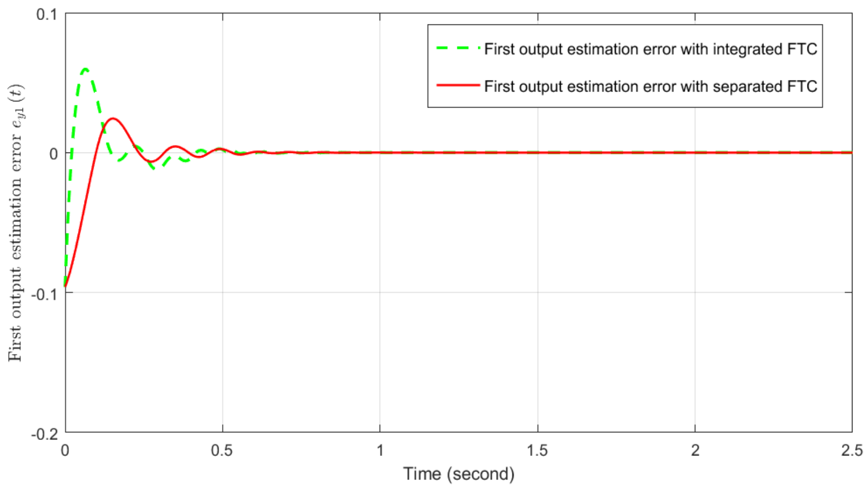

Figure 7. First output estimation error: First output estimation error with the separated FTC (red line) and the first output estimation error with the integrated FTC (green line).

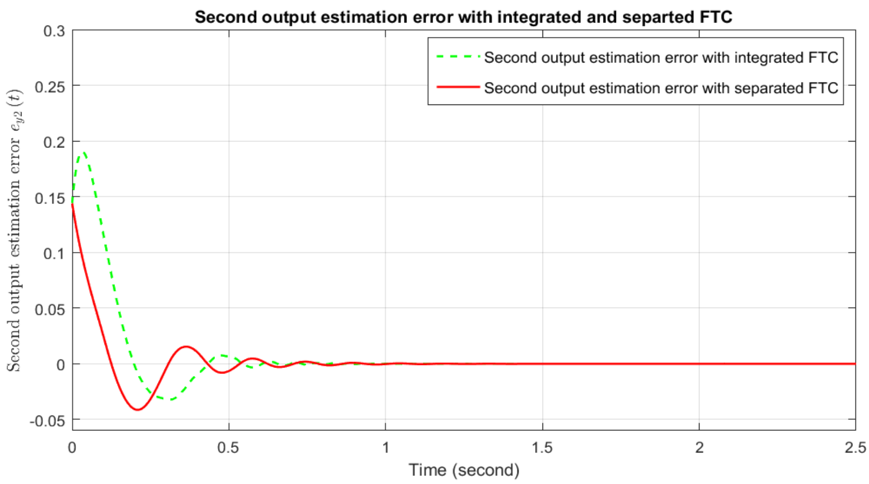

Figure 8. Second output estimation error: Second output estimation error with the separated FTC (red line) and second output estimation error with the integrated FTC (green line).

6.4. Simulation Result with a Different Constant Time Delay τ

In this section, in order to demonstrate the effectiveness of our method, we propose increasing the value of the time delay τ. Thus, Figure 9 shows the effect of increasing the constant τ on fault reconstruction using the integrated FTC design. In summary, increasing τ in a nonlinear LPV system with variable time-delay, particularly in scenarios involving actuator faults in diesel engines, can lead to performance degradation, stability issues, and increased control effort. However, employing integrated FTC strategies, including adaptive control, can effectively mitigate these adverse effects on fault reconstruction. By dynamically adjusting to increased time delays and compensating for actuator faults, FTC systems ensure that diesel engines operate reliably and efficiently, even under challenging conditions.

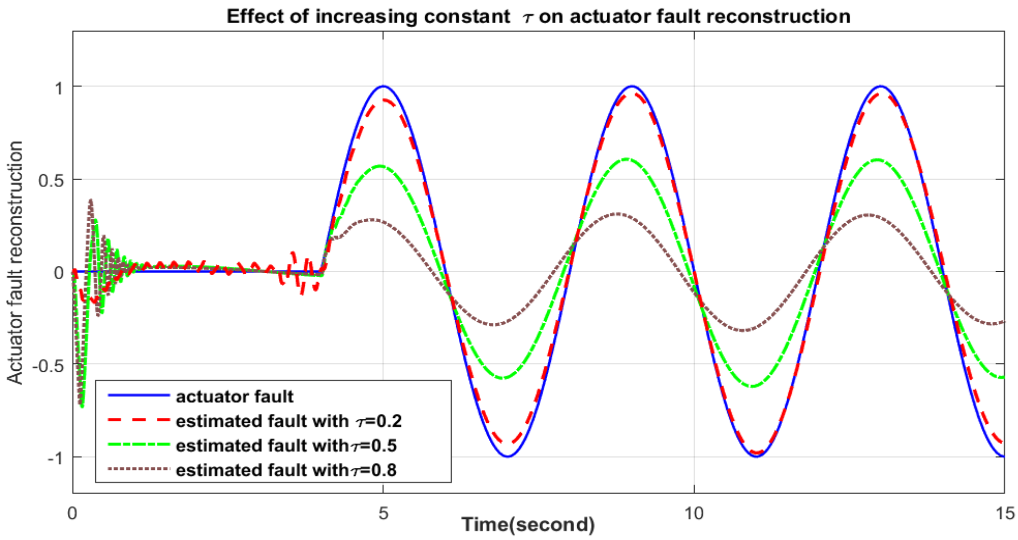

Figure 9. Effect of increasing constant τ on actuator fault reconstruction ($\tau = 0.2$ red line), ($\tau = 0.5$ green line), ($\tau = 0.8$ brown line).

6.5. Comparative Study

To validate the effectiveness of the proposed scheme, we present a comparative study with the control law used in [26]. The authors use a state feedback control law, which may have limited effectiveness when the system is affected by complex local nonlinearities such as the Lipchitz nonlinearity. In contrast, our SMC-based integrated FTC approach forces the system to remain on a sliding surface, thus guaranteeing stable performance even in the presence of unexpected variations in system parameters. Figure 10 shows the performance of our integrated SMC-based FTC on a sliding surface for the second scenario of actuator fault reconstruction when this fault changes its behavior.

The result shows that the SMC-based integrated FTC can adjust the control law according to variations in the system parameters, thus ensuring a rapid response (first response at t = 0.14 s). This contrasts with state feedback control, which is less effective in the face of these challenges (first response t = 0.19 s). From the zoomed-in version, it is clear that our adaptive controller is more robust against chattering effects than the state feedback-based controller.

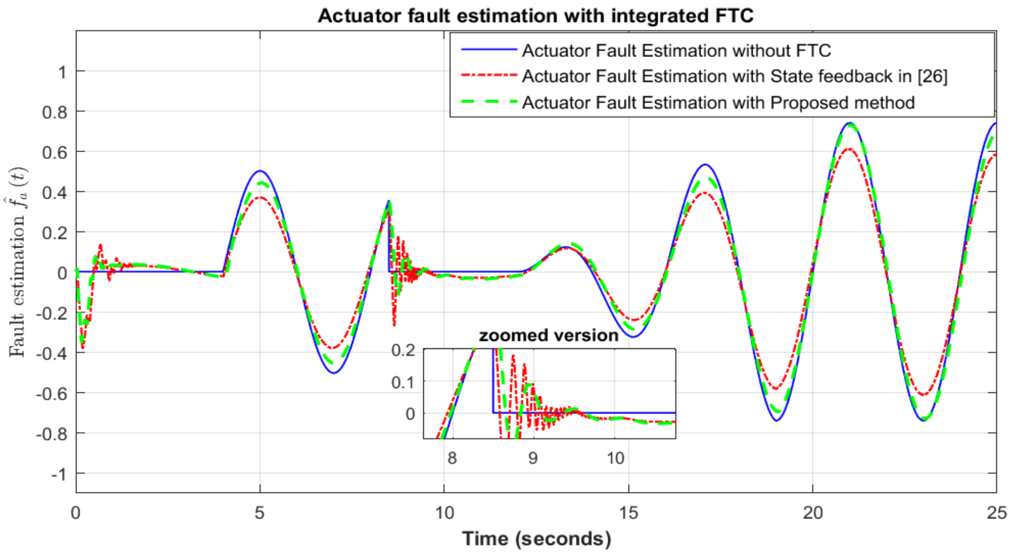

Figure 10. Actuator fault estimation without FTC (blue line), actuator fault estimation with state feedback in [26] (red line), and actuator fault estimation with the integrated FTC (green line).

Integrated FTC in the Presence of Measurement Noise

To demonstrate the effectiveness of the integrated FTC based on SMC compared to the state feedback-based controller used in [26], consider the influence of additive measurement noise on the system $\omega(t)$ to the output $y(t)$ with a variance of $10^{-5} \times I_2$ and zero mean.

Table 2 compares the proposed integrated FTC method with state feedback control in [26] with additional measurement noise. In addition, to evaluate the performance of the fault-tolerant control based on (SMC), the integral absolute error (IAE) on the output responses is used and the comparison results show that the best (IAE) is obtained by the FTC based on our proposed controller.

Table 2. IAE of outputs.

The Output $y(t)$	Integrated FTC-SMC	State Feedback in [26]
$y_1(t)$	0.049	0.071
$y_2(t)$	0.15	0.21

7. Conclusions

This paper tackles two significant challenges: firstly, the development of a fault estimation (FE) module utilizing a sliding mode observer scheme, and secondly, the implementation of fault estimation-based sliding mode fault-tolerant control for LPV delayed systems characterized by local nonlinear models. Initially, actuator faults are estimated through a robust adaptive sliding mode observer, which effectively handles norm-bounded uncertainties and variable time-delays. Sufficient conditions are derived to ensure the stability of the proposed observer, with H_∞ performance criteria aimed at minimizing the impact of uncertainties on the dynamics of estimation errors, which are solved through LMI optimization techniques. Subsequently, an adaptive fault-tolerant control strategy using output feedback is explored to mitigate the effects of actuator faults and ensure the stability of closed-loop nonlinear systems. The conditions for existence are formulated in terms of linear matrix inequalities (LMIs) using the Lyapunov–Krasovskii approach. In fact, by employing multi-objective convex optimization, the Lipschitz constant associated with the nonlinear terms of the LPV delayed model and the level of uncertainty attenuation are maximized simultaneously. This approach thus aids in determining the optimal gains for both the adaptive sliding mode observer and the controller. An integrated sliding mode FTC strategy is proposed to achieve optimal robustness through the interaction between the observer and controller models, offering several advantages over traditional separated FTC methods. Simulation results on a diesel engine system demonstrate the effectiveness of the proposed adaptive fault-tolerant control design based on actuator fault estimation, even in the presence of uncertainties and variable time-delay. As a perspective for future work, we plan to incorporate a compensation scheme to manage the significant delays and complex nonlinearities that occur in aerospace systems. This could include the use of advanced techniques such as delay observers or predictive controllers that anticipate the effects of delays.

Author Contributions: Conceptualization, O.M.; methodology, A.B.B.; formal analysis, A.B.B. and F.B.H.; investigation, O.M.; writing—original draft preparation: O.M.; writing–review and editing, A.B.B. and F.B.H.; A.B.B., F.B.H. and A.S. collaborated to achieve the work; A.S. led the project. All authors have read and agreed to the published version of the manuscript.

Funding: This research received no external funding.

Data Availability Statement: Data are contained within the article.

Conflicts of Interest: The authors declare no conflicts of interest.

References

1. Patel, H.R.; Shah, V.A. Shadowed type-2 fuzzy sets in dynamic parameter adaption in cuckoo search and flower pollination algorithms for optimal design of fuzzy fault-tolerant controllers. *Math. Comput. Appl.* **2022**, *27*, 89. [CrossRef]
2. Asadi, D. Model-based fault detection and identification of a quadrotor with rotor fault. *Int. J. Aeronaut. Space Sci.* **2022**, *23*, 916–928. [CrossRef]
3. Tayari, R.; Ben Brahim, A.; Ben Hmida, F.; Sallami, A. Active fault tolerant control design for lpv systems with simultaneous actuator and sensor faults. *Math. Probl. Eng.* **2019**, *2019*, 5820394. [CrossRef]
4. Ben Brahim, A.; Dhahri, S.; Ben Hmida, F.; Sellami, A. Multiplicative fault estimation-based adaptive sliding mode fault-tolerant control design for nonlinear systems. *Complexity* **2018**, *2018*, 1462594. [CrossRef]
5. Hmidi, R.; Ben Brahim, A.; Dhahri, S.; Ben Hmida, F.; Sellami, A. Sliding mode fault-tolerant control for Takagi-Sugeno fuzzy systems with local nonlinear models: Application to inverted pendulum and cart system. *Trans. Inst. Meas. Control.* **2021**, *43*, 975–990. [CrossRef]
6. Tan, J.; Zheng, H.; Meng, D.; Wang, X.; Liang, B. Active input design for simultaneous fault estimation and fault-tolerant control of LPV systems. *Automatica* **2023**, *151*, 110903. [CrossRef]
7. Quadros, M.M.; de Bessa, I.V.; Leite, V.J.; Palhares, R.M. Fault tolerant control for linear parameter varying systems: An improved robust virtual actuator and sensor approach. *ISA Trans.* **2020**, *104*, 356–369. [CrossRef]
8. Hmidi, R.; Brahim, A.B.; Hmida, F.B.; Sellami, A. Robust fault tolerant control design for nonlinear systems not satisfying matching and minimum phase conditions. *Int. J. Control Autom. Syst.* **2020**, *18*, 2206–2219. [CrossRef]
9. Zhang, W.; Xu, D.; Jiang, B.; Shi, P. Virtual-sensor-based model-free adaptive fault-tolerant constrained control for discrete-time nonlinear systems. *IEEE Trans. Circuits Syst. Regul. Pap.* **2022**, *69*, 4191–4202. [CrossRef]
10. Plata, C.; Prieto, P.J.; Ramirez-Villalobos, R.; Coria, L.N. Chaos synchronization for hyperchaotic lorenz-type system via fuzzy-based sliding-mode observer. *Math. Comput. Appl.* **2020**, *25*, 16. [CrossRef]
11. Serrano-Cruz, D.A.; Boutat-Baddas, L.; Darouach, M.; Astorga-Zaragoza, C.M.; Guerrero Ramírez, G.V. Modeling of the Human Cardiovascular System: Implementing a Sliding Mode Observer for Fault Detection and Isolation. *Math. Comput. Appl.* **2024**, *29*, 57. [CrossRef]
12. Heras-Cervantes, M.; Téllez-Anguiano, A.d.C.; Anzurez-Marín, J.; Espinosa-Juárez, E. Analysis and Comparison of Fuzzy Models and Observers for DC-DC Converters Applied to a Distillation Column Heating Actuator. *Math. Comput. Appl.* **2020**, *25*, 55. [CrossRef]
13. Feng, X.; Wang, Y. Fault estimation based on sliding mode observer for Takagi–Sugeno fuzzy systems with digital communication constraints. *J. Frankl. Inst.* **2020**, *357*, 569–588. [CrossRef]
14. Qi, H.; Shi, Y.; Li, S.; Tian, Y.; Yu, D.L.; Gomm, J. Fault tolerant control for nonlinear systems using sliding mode and adaptive neural network estimator. *Soft Comput.* **2020**, *24*, 11535–11544. [CrossRef]
15. Mousavi, S.M.M.; Ramezani, A. A new sliding mode observer design for fault estimation in a class of nonlinear fractional-order systems based on the super-twisting algorithm. *J. Control Autom. Electr. Syst.* **2021**, *32*, 1531–1539. [CrossRef]
16. Brahim, A.B.; Dhahri, S.; Hmida, F.B.; Sellami, A. Simultaneous actuator and sensor faults estimation design for LPV systems using adaptive sliding mode observers. *Int. J. Autom. Control* **2021**, *15*, 1–27. [CrossRef]
17. Lamouchi, R.; Raissi, T.; Amairi, M.; Aoun, M. On interval observer design for active Fault Tolerant Control of Linear Parameter-Varying systems. *Syst. Control Lett.* **2022**, *164*, 105218. [CrossRef]
18. Mabrouk, N.; Ben Brahim, A.; Ben Hmida, F. Simultaneous Multiplicative and Additive Actuator Faults Estimation-Based Sliding Mode FTC for a Class of Uncertain Nonlinear System. *Math. Probl. Eng.* **2023**, *2023*, 6902272. [CrossRef]

19. Wang, W.; Chen, J.; Huang, Z. Observer-Based State Estimation for Recurrent Neural Networks: An Output-Predicting and LPV-Based Approach. *Math. Comput. Appl.* **2023**, *28*, 104. [CrossRef]
20. Huang, Q.; Qi, J.; Dai, X.; Wu, Q.; Xie, X.; Zhang, E. Fault estimation method for nonlinear time-delay system based on intermediate observer-application on quadrotor unmanned aerial vehicle. *Sensors* **2022**, *23*, 34. [CrossRef]
21. Zhou, Y.; Ji, X. Static Output Feedback Control for Nonlinear Time-Delay Semi-Markov Jump Systems Based on Incremental Quadratic Constraints. *Math. Comput. Appl.* **2023**, *28*, 30. [CrossRef]
22. Kavikumar, R.; Sakthivel, R.; Kwon, O.; Kaviarasan, B. Faulty actuator-based control synthesis for interval type-2 fuzzy systems via memory state feedback approach. *Int. J. Syst. Sci.* **2020**, *51*, 2958–2981. [CrossRef]
23. Ahmed, S.; Azar, A.T.; Tounsi, M.; Ibraheem, I.K. Adaptive control design for Euler–Lagrange systems using fixed-time fractional integral sliding mode scheme. *Fractal Fract.* **2023**, *7*, 712. [CrossRef]
24. Ahmed, S.; Azar, A.T.; Ibraheem, I.K. Nonlinear system controlled using novel adaptive fixed-time SMC. *Aims Math.* **2024**, *9*, 7895–7916. [CrossRef]
25. Hamdi, H.; Rodrigues, M.; Mechmeche, C.; Braiek, N.B. Observer-based fault diagnosis for time-delay LPV descriptor systems. *IFAC-PapersOnLine* **2018**, *51*, 1179–1184. [CrossRef]
26. Hamdi, H.; Rodrigues, M.; Rabaoui, B.; Benhadj Braiek, N. A fault estimation and fault-tolerant control based sliding mode observer for LPV descriptor systems with time delay. *Int. J. Appl. Math. Comput. Sci.* **2021**, *31*, 247–258. [CrossRef]
27. Edwards, C.; Spurgeon, S.K. On the development of discontinuous observers. *Int. J. Control* **1994**, *59*, 1211–1229. [CrossRef]
28. Edwards, C.; Spurgeon, S. *Sliding Mode Control: Theory and Applications*; CRC Press: Boca Raton, FL, USA, 1998.
29. Edwards, C.; Spurgeon, S.K.; Patton, R.J. Sliding mode observers for fault detection and isolation. *Automatica* **2000**, *36*, 541–553. [CrossRef]
30. Ku, C.C.; Huang, K.W.; Chuang, S.Y. Gain-Scheduled Control of Delayed Diesel Engine System with Time-Varying Parameter. In Proceedings of the 2020 International Automatic Control Conference (CACS), Hsinchu, Taiwan, 4–7 November 2020; IEEE: New York City, NY, USA, 2020; pp. 1–6.